1-Benzopyran-4-one Antioxidants as Aldose Reductase Inhibitors

Luca Costantino,*[,†] Giulio Rastelli,[†] Maria Cristina Gamberini,[†] Joe A. Vinson,[‡] Pratima Bose,[‡] Anna Iannone,[§] Mariagrazia Staffieri,[§] Luciano Antolini,[⊥] Antonella Del Corso,[▽] Umberto Mura,[▽] and Albano Albasini[†]

Dipartimento di Scienze Farmaceutiche, Dipartimento di Scienze Biomediche, and Dipartimento di Chimica, Università di Modena, Via Campi 183, 41100 Modena, Italy, Department of Chemistry, University of Scranton, Scranton, Pennsylvania 18510-4626, and Dipartimento di Fisiologia e Biochimica, Università di Pisa,Via S. Maria 55, 56100 Pisa, Italy

Received July 27, 1998

Starting from the inhibitory activity of the flavonoid Quercetin, a series of 4*H*-1-benzopyran-4-one derivatives was synthesized and tested for inhibition of aldose reductase, an enzyme involved in the appearance of diabetic complications. Some of the compounds obtained display inhibitory activity similar to that of Sorbinil but are more selective than Quercetin and Sorbinil with respect to the closely related enzyme, aldehyde reductase, and also possess antioxidant activity. Remarkably, these compounds possess higher pK_a values than carboxylic acids, a characteristic which could make the pharmacokinetics of these compounds very interesting. Molecular modeling investigations on the structures of inhibitors bound at the active site of aldose reductase were performed in order to suggest how these new inhibitors might bind to the enzyme and also to interpret structure−activity relationships.

Introduction

Aldose reductase (alditol:NADP$^+$ oxidoreductase, E.C. 1.1.1.21, ALR2) is the first enzyme of the polyol pathway. Several experimental data link glucose metabolism through this pathway to long-term diabetic complications such as cataract, neuropathy, nephropathy, and retinopathy. Aldose reductase inhibitors (ARIs) should therefore be able to safely prevent or arrest the development of diabetic complications.

Among available orally active ARIs, two different chemical classes possessing an acidic proton have been reported: cyclic imides (spirohydantoins, such as Sorbinil) and carboxylic acid derivatives.[1−3] While their in vitro activity is similar, the in vivo activity is lower for carboxylic acids than for cyclic imides; in vivo, in the streptozotocin-induced diabetic rat, the most active carboxylic acids Tolrestat, Zopolrestat, and Zenarestat are active p.o. in reducing sorbitol levels in sciatic nerves with ED_{50} values of 4.8, 1.9, and 3.7 mg/kg, respectively;[3] Ponalrestat is active at the dose of 25 mg/kg;[3] the ED_{50} values for the lens are 18.4 mg/kg for Zopolrestat and 23 mg/kg for Zenarestat.[3] On the contrary, Sorbinil shows ED_{50} values in nerves and lens of 0.25 and 0.5 mg/kg, respectively.[2] The plasma half-life in man of Sorbinil (34−52 h) is markedly higher than that of carboxylic acids such as Tolrestat (10−11 h), Zenarestat (8 h), and Ponalrestat (13 h), the plasma half-life of Zopolrestat being the highest of this class of compounds (27.5 h).[3] A possible reason for this behavior in vivo could be that Sorbinil has higher pK_a values than carboxylic acids, with resultant better pharmacokinetic properties.[1,2] On the other hand, Sorbinil causes some hypersensitivity reactions,[2,4] and there is therefore a need for new ARIs with pK_a values higher than those of carboxylic acids.[2]

Moreover, besides enhancing the flow rate of the polyol pathway, hyperglycemia may induce pathological long-term complications in different ways,[5] among which oxidative stress may play a relevant role.[6] 4-Hydroxy-2,3-*trans*-nonenal (HNE), whose generation is enhanced in hyperglycemic conditions,[7,8] is one of the major toxic products of lipid peroxidation and exerts a marked effect on normal cell functions.[9] HNE is reduced by ALR2,[10,11] and inhibition of its metabolism by Sorbinil, a molecule devoid of antioxidant activity,[12] enhances its toxicity in vitro.[13,14] Moreover, in lenses cultured with HNE, the antioxidant Trolox prevents HNE-induced cataract, whereas Sorbinil, which is quite effective in preventing the development of hyperglycemic cataract, accelerates the progression of HNE-induced cataract.[15] ARIs possessing antioxidant activity would therefore seem to be desirable. On the other hand, ALR2 itself can be oxidatively modified to enzyme forms that are less sensitive to several ARIs,[16−18] which may affect their responsiveness to ARI therapy.

Naturally occurring flavonic compounds (2-phenyl-4*H*-1-benzopyran-4-one derivatives) are substances endowed with a large number of pharmacological activities. In particular, they are antioxidants and are able to inhibit ALR2.[19]

Many papers have appeared in the past reporting that flavonoids (such as glycosyl derivatives or aglycons) possess ALR2 inhibitory activity;[20−26] however, no definitive structure−activity relationships have been established, and the results indicating the importance of substituents present on the flavone nucleus seem somewhat controversial. Moreover, since at the time these studies were performed the crystal structure of ALR2 had not yet been solved, it was not clear how inhibitors might bind to the enzyme, and a structure-based approach was not possible.

* Address correspondence to Costantino Luca, Dipartimento di Scienze Farmaceutiche, Università di Modena. Tel: 0039 059 378554. Fax: 0039 059 378560. E-mail: albasini@unimo.it.
† Dipartimento di Scienze Farmaceutiche.
‡ University of Scranton.
§ Dipartimento di Scienze Biomediche.
⊥ Dipartimento di Chimica.
▽ Università di Pisa.

10.1021/jm980441h CCC: $18.00
Published on Web 05/11/1999

Table 1. Inhibitory Activity toward ALR2[a]

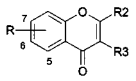

Comp.	R	R^2	R^3	ALR_2 IC50
1	5,7-OH		OH	32.87 (38.62-27.98)
2	5,7-OH		H	9.57 (11.50-7.96)
3	7-OH		H	6.52 (7.48-5.68)
4	7-OH		H	13.63 (16.58-11.21)
5	7-OH		H	14.65 (18.02-11.91)
6	5-OH		H	0% inh. at 39 μM
7	-		OH	0% inh. at 39 μM
8	7-OMe		H	32% inh. at 83 μM
9	7-OH	H	H	137 (157-119)
10	6,7-OH		H	3.98 (4.63-3.42)
11	6-NO_2, 7-OH		H	3.87 (4.74-3.16)
12b	7-OMe		H	0% inh. at 69 μM
12l	7-OH		H	7.01 (8.58-5.63)
12m	7-OH		H	6.61 (7.64-5.72)
13a	6-OH		H	13.12 (16.25-10.59)
13b	6-OMe		H	40% inh. at 72 μM
13c	7-OH		H	2.50 (2.98-2.09)
13d	7-OMe		H	37% inh. at 68 μM
13e	7-OH		H	41.01 (46.65-36.05)
13f	7-OH		H	29.35 (35.20-24.47)
13g	7-OH		H	3.14 (3.86-2.55)
13h	7-OH		H	10.89 (12.36-9.59)
13i	7-OH		H	22.27 (27.59-17.98
13l	7-OH			14.22 (15.96-12.5
13m	7-OH			0% inh. at 14 μM
14	7-COOH		H	10.89 (12.50-9.48)
15	7-OH	-CH_3		85.69 (105.42-69.65)
16	7-CH_2-COOH		H	1.30 (1.50-1.12)
17	7-OH	H		60.49 (71.07-51.48)
18	7-OMe	H		18% inh. at 77 μM

[a] IC_{50} (95% CL) (μM) or percent inhibition at a given concentration. Sorbinil: IC_{50} 1.85 (2.14−1.60) μM.

In our study, the lead compound is the aglycone ARI Quercetin (**1**) (Table 1). We started to simplify this molecule (compounds **2**−**9**, Table 1) in order to understand which part of the compound is most important for the inhibition of ALR2 and for selectivity. In fact, Quercetin is able to inhibit many enzymes, including aldehyde reductase (alcohol:$NADP^+$ oxidoreductase, E.C. 1.1.1.2, ALR1), a member of the aldo-keto reductase family sharing the highest homology in structure with ALR2. Although the physiological function of ALR1 is not completely understood, inhibitors should nevertheless not bind to this enzyme, to avoid side effects.[4] Thus, after having established the importance of the hydroxy group at position 7 of the benzopyrone nucleus, we synthesized and tested derivatives substituted also at position 2 and/or 3. The most interesting compounds here synthesized were tested as ARIs, ALR1 inhibitors, and antioxidants. On the basis of the results obtained, we also synthesized carboxylic acid derivatives of 4*H*-1-benzopyran-4-one, to compare their activity/selectivity with the most active phenolic compounds obtained.

To date, crystal structure investigations of complexes of ALR2 with carboxylic acid inhibitors such as Zopolrestat[27] and Tolrestat[28] or spirohydantoins (Sorbinil)[28] as well as modeling studies[29,30] have provided a description of the interactions of these compounds bound at the active site of ALR2. It is now of interest to investigate how our inhibitors, which are devoid of the carboxylic acid functional group, might interact with the enzyme. Therefore, a representative set of compounds was docked and energy-minimized in the ALR2 binding site, and the resulting structures were used to rationalize the structural features most important for inhibition and to provide a basis for discussion of structure−activity relationships in this class of compounds.

Chemistry

7-Hydroxy-2-(4′-hydroxyphenyl)-4*H*-1-benzopyran-4-one (**4**) and 7-hydroxy-6-nitro-2-phenyl-4*H*-1-benzopyran-4-one (**11**) (Table 1) were prepared starting from the reaction between the appropriate 2-hydroxyacetophenone and (substituted)benzoyl chloride in the presence of 3 and 4 equiv of LiHMDS,[31] respectively, followed by acid cyclization (Scheme 1); 7-methoxy-2-(4′-methoxyphenyl)-4*H*-1-benzpyran-4-one (**4a**) was then converted to **4** by treatment with HBr (48%).

The substituted 2-benzyl-4*H*-1-benzopyran-4-one derivatives **12a**−**o** were synthesized starting from the appropriate 2-hydroxyacetophenones **4b**−**d**,**g**−**i** or 4-substituted-2′-hydroxy-4′-methoxydihydrochalchones **4e**,**f** by reaction with the appropriate ester in the presence of NaH/pyridine (Scheme 1). The intermediate 1,3-diketones were then cyclized to **12a**−**o** with acetic acid/sulfuric acid. The structures of **12b**,**l**,**m** are shown in Table 1. The intermediates **12n**,**o** are shown in Scheme 2; in the cases of **12a**,**c**−**i**, only their chemical names have been reported in the Experimental Section. Treatment of **12a**−**i** with BBr_3 afforded the phenolic compounds **13a**−**m** (Table 1). A short reaction time afforded compounds still methoxylated at position 7 (**13d**) or 6 (**13b**) in the presence of the hydroxyl at position 4′. It was possible to synthesize the compound with a hydroxy group at position 7 together with a methoxy group at position 4′ (**12l**), starting from 2,4-dihydroxyacetophenone in which the 4-hydroxy group was protected as a tetrahydropyranyl derivative; the tetrahydropyranyl protecting group is easily removed during cyclization. Compound **14** was prepared (Scheme 2) starting from **12n**; treatment with CuCN followed by deprotection with BBr_3 and hydrolysis of the cyano group afforded **14**.

Compound **15** was prepared as described in Scheme 3. The acetylation of the dihydrochalcone **15a** afforded **15b** which, after rearrangement in basic conditions and subsequent cyclization in acidic medium, afforded **15c**. Deprotection with BBr_3 afforded **15**.

Compound **16** (Scheme 2) was prepared by treatment of **12o** with ethyl chloroformate to afford **16a**, which was

Scheme 1[a]

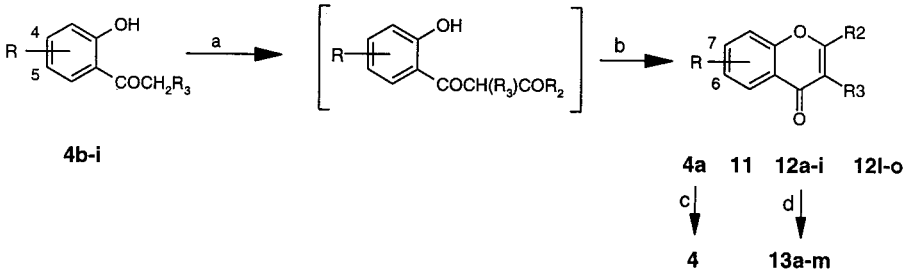

[a] (a) R_2COCl, LiHMDS for **4a** and **11**, R_2COOCH_3, NaH for **12a**−**o**; (b) CH_3COOH/H^+; (c) HBr (48%); (d) BBr_3.

Scheme 2[a]

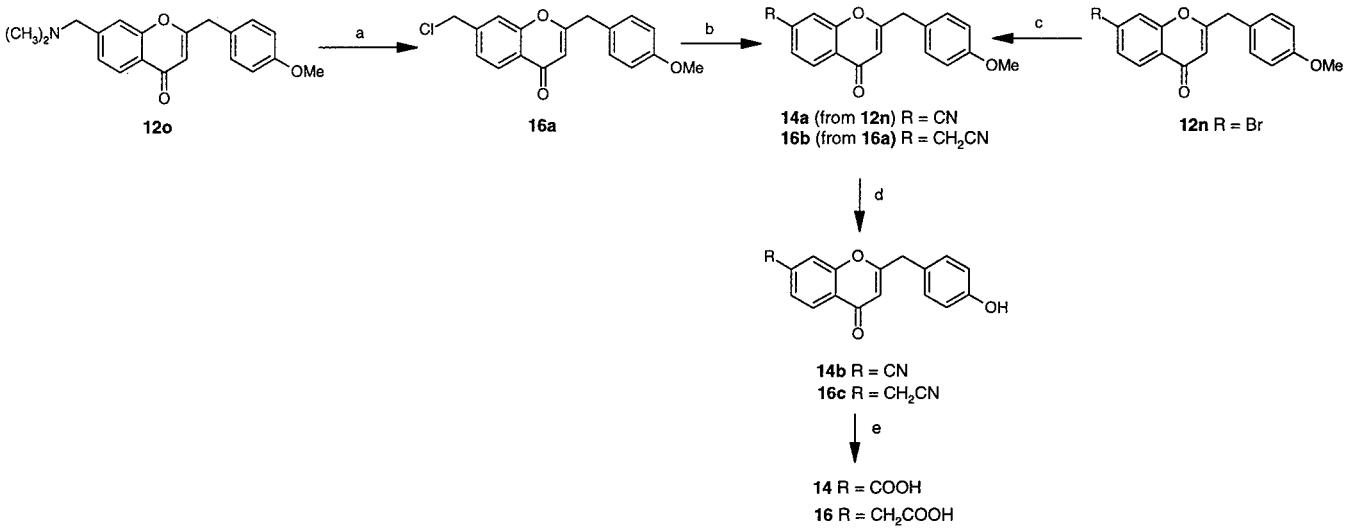

[a] (a) ClCOOEt; (b) KCN, DMSO; (c) CuCN, DMF; (d) BBr_3; (e) H_2SO_4 (70%).

Scheme 3[a]

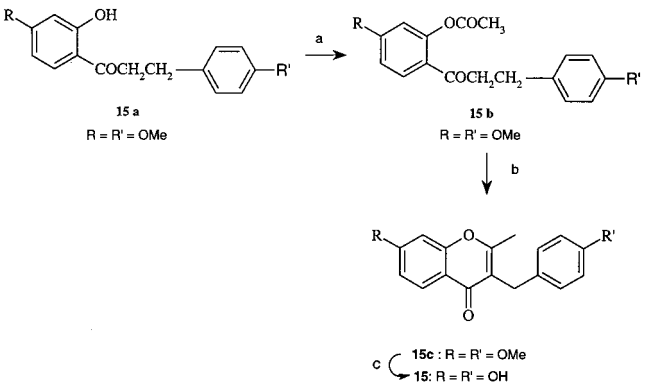

[a] (a) $N(Et)_3$/DMAP, CH_3COCl; (b) (1) NaH, DMSO, (2) CH_3COOH/H^+; (c) BBr_3.

converted to **16b** by treatment with KCN in DMSO. Deptotection of the phenolic hydroxyl group with BBr_3 and subsequent hydrolysis of the nitrile afforded **16**.

3-Substituted-4*H*-1-benzopyran-4-ones **17** and **18** (Table 1) were obtained by treatment of 2,4,4′-trihydroxydihydrochalcone[32] with boron trifluoride−diethyl etherate, followed by reaction with methanesulfonyl chloride, as described in the general method.[33] **17**, thus obtained, was converted into **18** by treatment with diazomethane.

Results and Discussion

Biology. Starting from Quercetin (**1**), the minimum requirement for inhibition of ALR2 (Table 1) was established as being the presence of the 7-hydroxyl and the phenyl at position 2 of the benzopyrone nucleus. The importance of the hydroxy group in position 7 emerged from the study of the activity of compounds **5**−**8**. While compound **5**, which bears only the 7-hydroxyl, is still active (IC_{50} 14.65 μM), the corresponding methoxylated compound **8** is considerably less active (32% inhibition at 83 μM) (Table 1). Compounds **6** (with an OH at position 5) and **7** (OH at position 3) are inactive at the solubility limit in the assay mixture (39 μM). Given that the pK_a value (7.30[34]) of compound **5** approaches the pH of the enzymatic assay, these compounds probably act in their anionic forms, in line with the general view[2,4] regarding the importance of the presence of anionic forms on the inhibition of ALR2. In support of this hypothesis, the methoxylated compound **8**, in which proton dissociation is prevented, is found to be much less active than **5**. Moreover, the pK_a values of hydroxy groups at positions 5 and 3 of the benzopyrone nucleus are much higher, resulting in less acidic compounds (pK_a = 11.6[35] and 9.75,[36] respectively). The introduction of an additional hydroxy group (compound **10**) or a nitro group (compound **11**) at position 6 of compound **5** led to more acidic compounds (Table 3), 3 times more active than **5**.

As regards the importance of the 2-phenyl moiety, compound **9**, in which the phenyl group was removed, is 10 times less active than **5** (IC_{50} 137 μM vs 14.65 μM for compounds **9** and **5**, respectively). Therefore, an aromatic substituent in this position is important for activity. Thus, while maintaining the hydroxy group at

Table 2. Inhibitory Activity toward ALR2 and ALR1[a]

compd	IC_{50} ALR2	IC_{50} ALR1	IC_{50}(ALR1)/ IC_{50}(ALR2)
1	32.87 (38.62−27.98)	10.34 (12.57−8.50)	0.3
5	14.65 (18.02−11.91)	45.21 (51.91−39.38)	3.1
9	137 (157−119)	114 (128−101)	1.0
11	3.87 (4.74−3.16)	27.5% inhib at 91 μM	
12l	7.01 (8.58−5.63)	16.63 (19.86−13.93)	2.4
12m	6.61 (7.64−5.72)	39.17 (44.05−34.83)	5.9
13c	2.50 (2.98−2.09)	16.78 (18.40−15.30)	6.7
13g	3.14 (3.86−2.55)	13.23 (15.80−11.26)	4.2
16	1.30 (1.50−1.12)	128 (149−110)	98.5
Sorbinil	1.85 (2.14−1.60)	1.56 (1.91−1.27)	0.8

[a] IC_{50} (95% CL) (μM) or percent inhibition at a given concentation.

Table 3. pK_a Values (25 °C) of Selected Compounds

compd	pK_a (±SD)
10	6.85 (0.09)
11	5.30 (0.12)
12l	7.35 (0.07)
13a	8.89 (0.03)

position 7, we synthesized and tested derivatives substituted at position 2 and/or 3 (Table 1). Of the phenolic compounds synthesized, the best compound is **13c**, with an ALR2 IC_{50} value of the same order of magnitude as that of Sorbinil, accompanied by a 10-fold increase in selectivity with respect to ALR1 (Table 2). The methylation of the 7-hydroxyl causes a drastic reduction in activity (compound **13d**), while that of the 4′-OH (compound **12l**) causes only a 3-fold decrease in activity; the same occurs if the 4′-hydroxybenzyl group is at position 3 of the benzopyrone nucleus (compounds **17** and **18**). The methylation of both hydroxyls of **13c** (compound **12b**) leads to a completely inactive compound.

To investigate the differences between phenolic and carboxylic acid derivatives of the 4*H*-1-benzopyran-4-one nucleus, we synthesized compounds carrying a carboxy group at position 7. While the substitution of the 7-hydroxyl in compound **13c** with a carboxylic group (compound **14**) causes a reduction in activity, the higher homologue (compound **16**) is found to exert the same activity as compound **13c**, along with an increase in selectivity: ALR2 is inhibited 2 orders of magnitude more than ALR1.

Moving the hydroxy group from position 7 to 6 (compound **13a**) causes a decrease in inhibitory activity; this finding can be attributed to an increase in the pK_a value (pK_a of **13a** is 8.89 vs pK_a of 7.35 for **12l**) (Table 3). The fact that the corresponding methoxy derivative **13b** is much less active suggests that compound **13a** is also likely to act in its anionic form.

The most interesting compounds, **13a**,**c**,**g**, which are more selective than Sorbinil and are only partially ionized at the pH of the enzymatic assay (pH 6.80), also possess antioxidant activity in AAPH-induced peroxidation of liposomes (Table 4), even if less potently than BHT. **13c**,**g** were also evaluated as antioxidants in a VLDL + LDL lipoprotein oxidation model, which simulates the oxidation mechanism of atherogenesis.[37] While **13c** has an IC_{50} value of 1.59 μM, **13g** is more active (IC_{50} 0.10 μM); in the same assay, BHT and Quercetin display IC_{50} values of 0.27 and 0.22 μM, respectively.

Molecular Modeling. Three compounds were selected for computational analysis, namely, **13c**, **4**, and **16** (Table 1). They are among the most active ARIs developed in this study and were chosen to represent the most active members of the 7-hydroxy-4*H*-1-benzopyran-4-one derivatives with a 2-benzyl substituent (inhibitor **13c**), a 2-phenyl substituent (inhibitor **4**), and a carboxylic derivative (**16**).

It is known from the crystal structures of complexes of ALR2 with carboxylic acid inhibitors[27,28] and from molecular modeling studies[29,30,38] that carboxylic acid derivatives bind ALR2 with the carboxylate function interacting with Tyr48, His110, and Trp111, which are three key residues in binding and catalysis.[39,40] Accordingly, inhibitor **16** is expected to bind ALR2 with its carboxylate in a similar position. As for inhibitors **13c** and **4**, the acidic nature of the hydroxyl at position 7 (pK_a 7.30[34]) is fundamental to the inhibition of ALR2. Indeed, methylation of the 7-hydroxyl, which prevents dissociation, leads to completely inactive compounds. This finding gives a clear indication that 7-hydroxy flavones exert their inhibitory activity toward ALR2 in their anionic, dissociated form and that the anionic form produced by dissociation of this hydroxyl could resemble the carboxylate function of inhibitor **16**. For this reason, inhibitors **13c** and **4** are considered as dissociated (anionic) in the docking and molecular mechanics calculations presented below.

Two different structures of ALR2 have been considered for the modeling of the structures of the ALR2−inhibitor complexes. In fact, it is known from previous crystallographic[27,28] and modeling[29,30,38] studies that the binding of inhibitors to ALR2 induces significant conformational changes in the enzyme. In particular, conformational changes of a loop (residues 121−135) and a short segment (residues 298−303) of the enzyme have been linked to the opening of an additional

Table 4. Antioxidant Action of ARIs Tested in AAPH-Induced Peroxidation of Liposomes

	nmol of MDA/mL ± SE (no. of experiments)				
	5 min	15 min	30 min	40 min	60 min
control	1.422 ± 0.252 (5)	2.250 ± 0.120 (5)	2.704 ± 0.165 (5)	2.922 ± 0.203 (4)	4.079 ± 0.437 (5)
13a	1.188 ± 0.072 (4)	1.543 ± 0.332 (4)	1.460 ± 0.224[a] (4)	1.292 ± 0.222[a] (4)	1.269 ± 0.154[b] (6)
13c	2.020 ± 0.205 (3)	1.950 ± 0.102 (3)	1.895 ± 0.338[a] (4)	2.097 ± 0.247[a] (3)	1.811 ± 0.258[b] (4)
13g	0.935 ± 0.325 (4)	1.180 ± 0.093[b] (4)	1.067 ± 0.128[b] (4)	0.852 ± 0.299[b] (4)	1.528 ± 0.399[b] (4)
BHT	1.625 ± 0.435 (3)	1.328 ± 0.267[b] (3)	1.326 ± 0.096[b] (3)	1.227 ± 0.0197[b] (3)	0.937 ± 0.243[b] (3)

[a] $p < 0.05$ with respect to control. [b] $p < 0.01$ with respect to control.

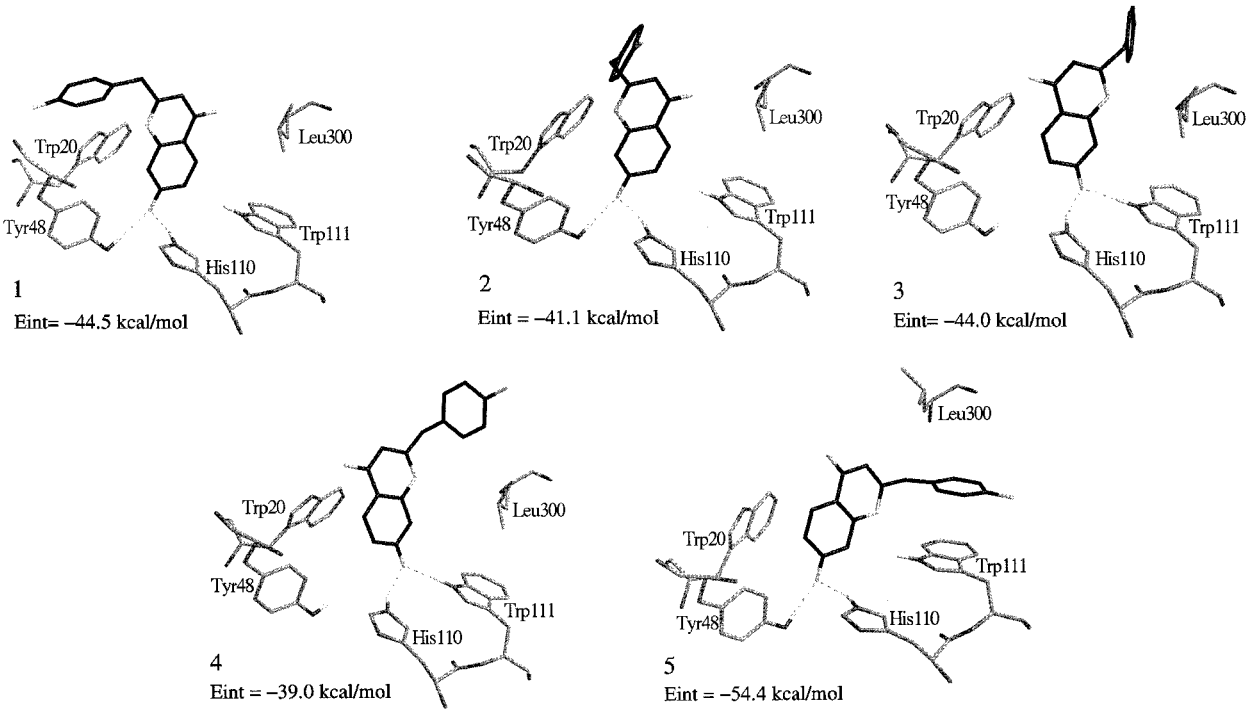

Figure 1. Orientations of inhibitor **13c** with respect to selected amino acid residues composing the active site of ALR2 and interaction energies (kcal/mol) of the inhibitor with the protein.

hydrophobic pocket, which is completely closed in the structure of the apoenzyme and which binds hydrophobic aromatic substituents of inhibitors such as benzothiazoles. The binding of inhibitors inside this pocket provides very active and selective inhibitors with respect to ALR1. Since, in addition to the ionizable 7-acetic acid or 7-hydroxyl functions attached to the benzopyrone nucleus, our inhibitors possess a hydrophobic aromatic substituent at position 2, we wished to determine whether this substituent binds inside or outside this pocket. Accordingly, two structures of ALR2 were used: the crystal structure of the apoenzyme[41] (closed hydrophobic pocket) and the structure of ALR2 obtained after docking and energy minimization of a bulky inhibitor specifically designed to fit into the hydrophobic pocket with a benzothiazole substituent[38] (open hydrophobic pocket). The latter structure is very similar to the crystal structure of ALR2 complexed with the potent inhibitor Zopolrestat,[27] whose coordinates are still not available.

A novel strategy was devised for the modeling of the complexes. First, initial orientations of the inhibitor in the ALR2 binding site were assessed using DOCK 3.5. DOCK retrieves families of orientations of inhibitors in the binding cleft and scores them on the basis of the interaction energy with the protein (sum of electrostatic and van der Waals interactions). Generally, these orientations cluster into families. However, since DOCK does not allow conformational changes of ligands and enzyme upon formation of the complex, i.e., it is rigid, energy-minimization of the complexes with molecular mechanics was performed to allow conformational changes. In this study, all orientations within a 10 kcal/mol energy interval from the most attractive orientation found by DOCK were saved, and each significantly different orientation was then optimized using AMBER 4.1.

Energy minimization of the complexes, in which both the inhibitor and a significantly large portion of ALR2 were allowed to move, is particularly important in the most conformationally flexible regions of the active site, like those of the open hydrophobic pocket. In fact, the starting structure we used for modeling was obtained after docking and energy minimization of an inhibitor that fits the hydrophobic pocket with a benzothiazole substituent, while the inhibitors here reported possess a phenyl substituent. Therefore, energy minimization was necessary to allow conformational changes and to correctly account for differences in binding benzothiazole and phenyl substituents in this important region of the active site. Finally, molecular modeling simulations of the structure of the complex of ALR2 and Tolrestat[29] (which has a hydrophobic substituent different from both benzothiazole and phenyl and were found to bind in a rather different orientation and with different conformational changes of the hydrophobic pocket) were found to reproduce closely the crystal structure of the complex solved later.

To estimate and compare the strength of the interactions and to select the most favorable orientations in the binding cleft, the interaction energies of the inhibitors with the enzyme in each case were calculated. In addition, for the more conformationally flexible inhibitors, **13c** and **16**, the two conformations in which the 2-benzyl is perpendicular to the benzopyrone ring (owing to the presence of the methylene spacer) but pointing in opposite directions were both considered for docking. These two conformations are almost energetically equivalent in vacuo but lead to significantly different orientations inside aldose reductase.

Figure 1 reports the energy-minimized structures of the complexes of inhibitor **13c** with aldose reductase for each orientation retrieved by DOCK, together with the interaction energies of the inhibitor with the protein

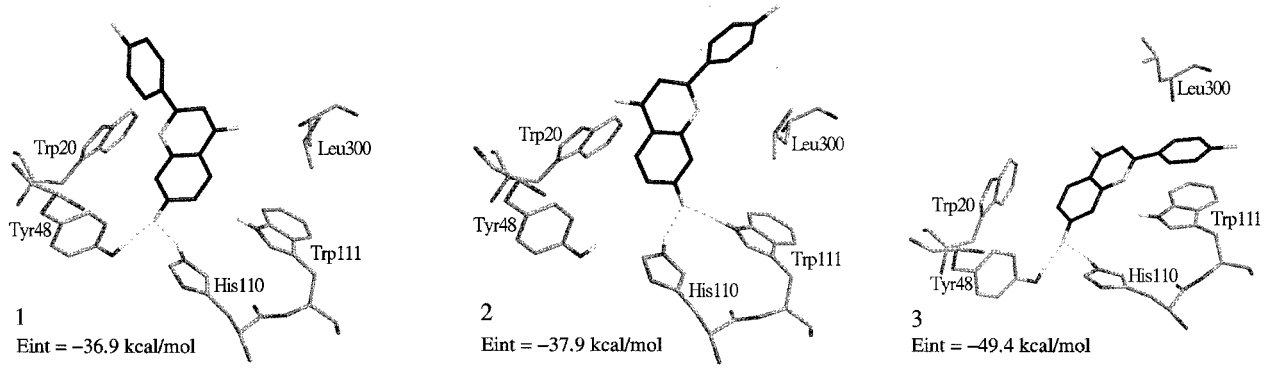

Figure 2. Orientations of inhibitor **4** with respect to selected amino acid residues composing the active site of ALR2 and interaction energies (kcal/mol) of the inhibitor with the protein.

calculated using the AMBER force field. In all orientations, the dissociated hydroxyl at position 7 of inhibitor **13c** interacts with Tyr48, His110, Trp111, and the positively charged nicotinamide ring of $NADP^+$. This result is of particular importance because it rationalizes the need for a dissociated free hydroxyl at position 7 revealed by structure−activity relationships: intriguingly, this dissociated hydroxyl interacts with the most important residues of the active site and replaces the carbonyl oxygen of the aldehyde substrates,[42] being hydrogen bonded to the same residues and within 3.1 Å from the reactive C4 of the nicotinamide ring of the cofactor. Furthermore, the dissociated hydroxyl at position 7 effectively resembles the carboxylate functional group of several carboxylic acid inhibitors of ALR2 that have been reported to date, on account of its ability to bind Tyr48 and His110. In orientations 1 and 2, the O7 of the inhibitor hydrogen bonds to Tyr48 and His110 and the 2-benzyl substituent points in opposite directions, owing to the two different allowed conformations of the inhibitor. In orientations 3 and 4, O7 hydrogen bonds to His110 and Trp111 and again the 2-benzyl substituent points in opposite directions. Compared with orientations 1 and 2, orientations 3 and 4 differ on account of an almost 180° rotation of the benzopyrone ring. Orientation 5 was found for the open form of the additional hydrophobic pocket mentioned above. In this orientation, O7 still interacts with Tyr48 and His110, but the 2-benzyl substituent fits into the open hydrophobic pocket. This orientation is largely favored over orientations 1−4, the interaction energy being about 10 kcal/mol more attractive in this case. Therefore, inhibitor **13c** probably binds aldose reductase by adopting orientation 5, which combines strong interactions of the dissociated hydroxyl at position 7 with the two hydrogen bond donors Tyr48 and His110 with strong interactions of the 2-benzyl substituent with the additional hydrophobic pocket. Worthy of note is that only one orientation (5) was found to fit into the open form of the enzyme, at variance with the closed form of the enzyme, where four different, less stable and probably less specific, orientations were found.

The finding that inhibitor **13c** fits into the additional hydrophobic pocket lined by Trp111 and Leu300 has important consequences for the selectivity of the inhibitor for ALR2 with respect to ALR1. In fact, these two enzymes differ mainly for the residues composing the hydrophobic pocket, the rest of the enzyme being highly conserved.[28,43] Inhibitors able to bind in this pocket have been reported to be selective for ALR2.[28] The finding that inhibitor **13c** binds in the hydrophobic pocket accounts for the selectivity observed for this inhibitor. Intriguingly, 7-hydroxybenzopyrone itself (compound **9**), which lacks the 2-benzyl substituent, is not at all selective for ALR2, evidently because it lacks the aromatic substituent that fits into the specificity pocket. Besides specificity, the finding that this inhibitor is considerably less active than **13c** for the inhibition of ALR2 demonstrates that the interactions between the 2-benzyl substituent and the hydrophobic pocket are important for the affinity of inhibitors.

Figure 2 reports the optimized structures found for inhibitor **4**. As in the case of inhibitor **13c**, the dissociated hydroxyl at position 7 interacts with Tyr48, His110, and Trp111 in all orientations, thus providing further evidence of the importance of this functional group for inhibitor binding to ALR2. In orientation 1, the O7 hydrogen bonds to Tyr48 and His110, while in orientation 2, the O7 hydrogen bonds to His110 and Trp111. These two orientations differ mainly by virtue of a 180° rotation of the benzopyrone ring. Orientation 3 was obtained from the open structure of the hydrophobic pocket. Remarkably, this orientation exhibits an 11 kcal/mol more favorable interaction energy with the enzyme than orientation 2 and is therefore largely preferred. In orientation 3, O7 hydrogen bonds to Tyr48 and His110, and the 2-phenyl ring fits into the open hydrophobic pocket. Therefore, despite the lack of the methylene spacer at position 2, one can still predict that inhibitor **4** will fit into the hydrophobic pocket.

The last inhibitor considered was **16**, the derivative of inhibitor **13c**, in which the 7-hydroxyl was replaced by an acetic acid chain. The orientations found for this inhibitor are reported in Figure 3. All orientations show the carboxylate function close to Tyr48, His110, and Trp111, in agreement with crystal structures of other carboxylic acid inhibitors and previous molecular modeling calculations. Orientations 1 and 2, in which one oxygen of the carboxylate hydrogen bonds to Tyr48 and His110, differ in the rotation of the 2-benzyl substituent. In orientation 3, one oxygen of the carboxylate hydrogen bonds to His110 and Trp111, while the rest of the inhibitor points in the opposite direction from orientations 1 and 2. The latter orientation shows the carboxylate hydrogen bonded to Tyr48, His110, and Trp111 and the 2-benzyl substituent inserted in the open hydrophobic pocket (orientation 4). Again, this orientation is

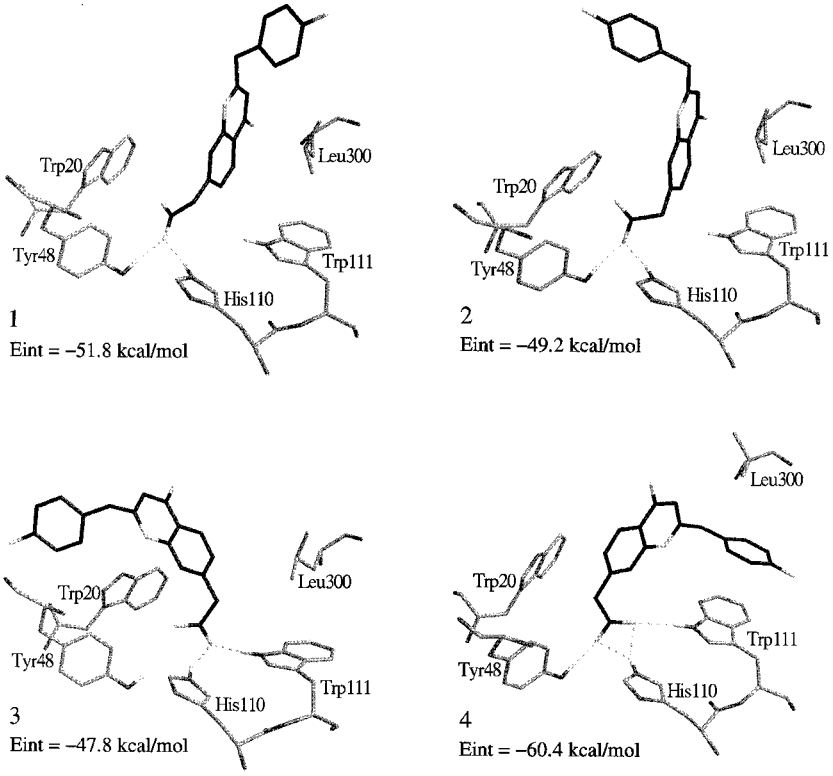

Figure 3. Orientations of inhibitor **16** with respect to selected amino acid residues composing the active site of ALR2 and interaction energies (kcal/mol) of the inhibitor with the protein.

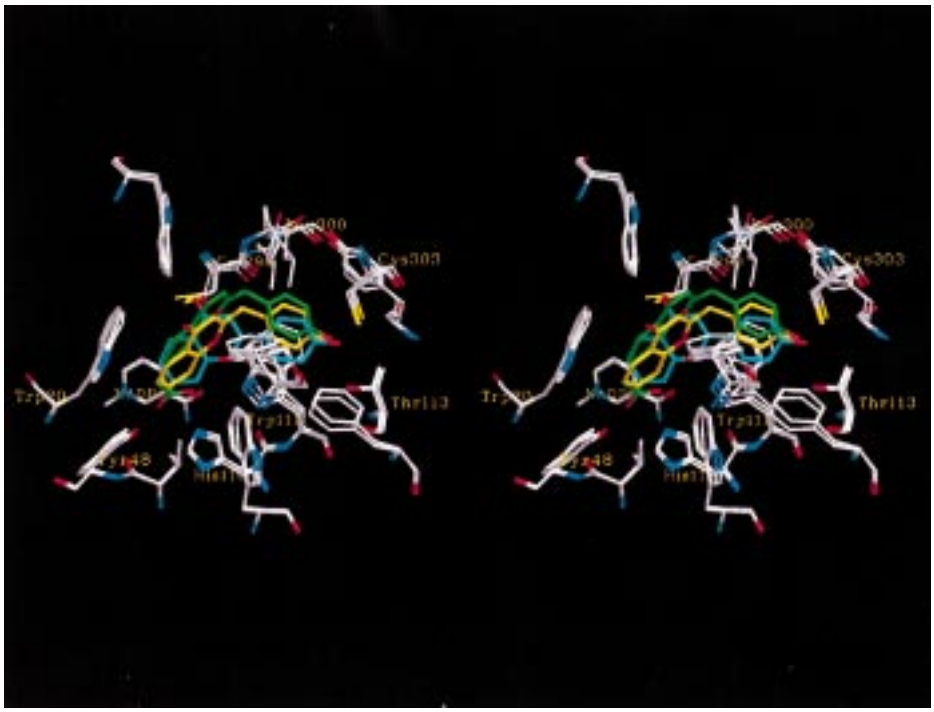

Figure 4. Superposition of the structures of inhibitors **13c** (yellow), **4** (cyan), and **16** (green) bound at the active site of ALR2 (stereoview). The most favorable orientations for each inhibitor have been superimposed.

strongly preferred over the others, being about 9 kcal/mol more attractive than orientation 1.

In summary, the modeling of ALR2−inhibitor complexes predicts that the dissociated hydroxyl at position 7 of inhibitors **13c** and **4** effectively binds the Tyr48/His110 catalytic residues, thus providing a good structural replacement for the carboxylate functional group of inhibitor **16** and of a huge series of carboxylic acid inhibitors of ALR2 developed to date. In Figure 4 we present the superimposition of the final structures of the complexes of inhibitors **13c**, **4**, and **16** with ALR2 in their most favored orientations. As inferred from the superimposition, all inhibitors nicely complement the active site architecture. In addition to the interactions established with Tyr48 and His110, all inhibitors bind the 2-phenyl substituent in the hyrophobic pocket, thus

enhancing inhibitory activity for ALR2 and selectivity with respect to ALR1. Structures can also easily explain why, starting from Quercetin which is highly hydroxylated, removal of the hydroxyls at positions 3, 5, and 3′ leads to progressive enhancement of inhibitory activity. In fact, apart from Tyr48 and His110, which interact with O7, the other residues directly in contact with inhibitors **13c**, **4**, and **16** are predominantly hydrophobic in nature (Figure 4) and are not apt to give hydrogen bonds with these hydroxyls. From structure−activity analysis of the data in Table 1, the only hydroxyl that leads to an increase in inhibitory activity is that in position 4′, which is coherently found to hydrogen bond to Thr113 (Figure 4).

Experimental Section

Chemistry. UV−vis spectra were obtained by means of a Perkin-Elmer spectrophotometer mod λ 16 equipped with a thermostated cuvette holder. Melting points were determined on a Buchi 510 melting point apparatus and are uncorrected. ^{1}H NMR spectra were recorded on a Bruker AC200 spectrometer (Centro Interdipartimentale Grandi Strumenti, Modena University). Unless otherwise stated, spectra were recorded in DMSO-d_6. Chemical shifts are reported in ppm from tetramethylsilane as internal standard. *J* values are given in Hz. Microanalyses were carried out in the microanalysis Laboratory of the Dipartimento di Scienze Farmaceutiche, Modena University. Analyses indicated by the symbols of the elements were within ±0.4% of the theoretical values. TLC was performed on precoated silica gel F254 plates (Merck). Silica gel (Merck, 70−230 mesh) was used for column chromatography. The methyl esters were obtained from the corresponding acids by reaction with diazomethane in methanolic solution. Petroleum ether (bp 60−80 °C) was used. Quercetin (**1**) was purchased from Fluka, 5,7,3′,4′-tetrahydroxyflavone (**2**), 7,3′,4′-trihydroxyflavone (**3**), and 6,7-dihydroxyflavone (**10**) were from Extrasynthese; 7-hydroxyflavone (**5**), 5-hydroxyflavone (**6**), and 3-hydroxyflavone (**7**) were from Roth. 7-Hydroxy-4*H*-1-benzopyran-4-one (**9**) was prepared following the procedure reported in ref 44. 7-Methoxyflavone (**8**) was prepared from 7-hydroxyflavone by reaction with diazomethane in acetone solution (mp 110−2, 111.5−2.5 °C[45]).

7,4′-Dimethoxy-2-phenyl-4*H*-1-benzopyran-4-one (4a). A solution of lithium bis(trimethyl)silylamide (LiHMDS) in THF (1 M, 18.0 mL, 18.0 mmol) was slowly added (15 min) to a well-stirred solution of 2-hydroxy-4-methoxyacetophenone (**4b**) (1.00 g, 6.0 mmol) in THF (50 mL) under a nitrogen atmosphere at −78 °C. The reaction mixture was further stirred at −78 °C for 1 h and then at 0 °C for 2 h. It was then cooled again to −78 °C, and a solution of 4-methoxybenzoyl chloride (1.00 g, 6.0 mmol) in THF (20 mL) was added. Stirring was continued for 30 min at −78 °C and then at room temperature for 4 h. The reaction mixture was poured into water and ice (250 mL) and HCl (10 mL). It was extracted with $CHCl_3$ (3 × 25 mL), and the combined extracts were dried (Na_2SO_4). The solvent was evaporated and the residue mixed with acetic acid (50 mL) and sulfuric acid (0.25 mL) and heated at 100 °C for 1 h. After cooling the reaction mixture, water (50 mL) was added, and the resulting precipitate was collected and washed with water: yield 1.40 g (82%); mp 138−40 °C (lit. mp 144−6 °C[46]); ^{1}H NMR 8.20 (2H, m), 7.90 (1H, d, J = 8.78), 7.32 (1H, d, J = 2.30), 7.14 (2H, m), 7.07 (1H, dd, J = 8.78, J = 2.30), 6.86 (1H, s), 3.94 (3H, s), 3.88 (3H, s).

7,4′-Dihydroxy-2-phenyl-4*H*-1-benzopyran-4-one (4). A suspension of **4a** (0.30 g, 1.06 mmol) in HBr 48% (12 mL) was heated at reflux for 15 h; the resulting reaction mixture was cooled and the precipitate collected and washed with water. Crystallization from methanol/acetone afforded **4**: yield 0.13 g (48%); mp 308−10 °C (lit. mp 310−1 °C[47]); ^{1}H NMR 10.70 (1H, s), 10.20 (1H, s), 7.89 (3H, m), 6.99 (4H, m), 6.71 (1H, s). $C_{15}H_{10}O_4$: C, H.

7-Hydroxy-6-nitro-2-phenyl-4*H*-1-benzopyran-4-one (11). A solution of LiHMDS in THF (1 M, 24.0 mL, 24.0 mmol) was added to a solution of 2,4-dihydroxy-5-nitroacetophenone (**4c**)[48] (1.20 g, 6.1 mmol). The procedure was then the same as for **4a**, using benzoyl chloride (0.71 mL, 6.1 mmol): yield 0.72 g (42%); mp 220−2 °C (acetone); ^{1}H NMR 12.24 (1H, s), 8.48 (1H, s), 8.10 (2H, m), 7.60 (3H, m), 7.32 (1H, s), 7.02 (1H, s). $C_{15}H_9NO_5$: C, H, N.

General Procedure for the Synthesis of Compounds 12a−n. A solution of the appropriate 2-hydroxyacetophenone (4.0 mmol) and the appropriate methyl ester (4.4 mmol) in anhydrous pyridine (8 mL) was added dropwise to a well-stirred suspension of NaH (60% dispersion in mineral oil) (12 mmol) in anhydrous pyridine (8 mL). When the reaction subsided, the mixture was heated at 90 °C for 15 min. After cooling, the mixture was decomposed in 2 N HCl and extracted with methylene chloride (3 × 25 mL). The combined organic layers were washed with 1 N HCl (2 × 30 mL) and water (30 mL) and dried (Na_2SO_4), and the solvent was removed under reduced pressure. The residue was then dissolved in acetic acid (20 mL) and concentrated sulfuric acid (0.1 mL). In the case of 2-hydroxy-4-(2-tetrahydropyranyloxy)acetophenone starting material (for **12l**, **m**), a solution of acetic acid (20 mL) and concentrated HCl (1.5 mL) was used. The resulting solution was then heated at 100 °C for 30 min. After cooling, the solution was concentrated under reduced pressure; then water was added (50 mL). The mixture was then extracted with ethyl acetate (3 × 25 mL), the organic layer was dried (Na_2SO_4), and the solvent was removed under reduced pressure. The residue was then purified by means of column chromatography (cyclohexane:EtOAc, 75:25) and crystallized from acetone/petroleum ether.

6-Methoxy-2-(4′-methoxybenzyl)-4*H*-1-benzopyran-4-one (12a) was synthesized by reaction between 2-hydroxy-5-methoxyacetophenone (**4d**) and methyl 4-methoxyphenylacetate: yield 57%; mp 71−2 °C; ^{1}H NMR ($CDCl_3$) 7.56 (1H, d, J = 2.93), 7.36 (1H, d, J = 8.96), 7.25 (3H, m), 6.95 (2H, m), 6.13 (1H, s), 3.90 (3H, s), 3.88 (2H, s), 3.83 (3H, s).

7-Methoxy-2-(4′-methoxybenzyl)-4*H*-1-benzopyran-4-one (12b) was synthesized by reaction between 2-hydroxy-4-methoxyacetophenone (**4b**) and methyl 4-methoxyphenylacetate: yield 56%; mp 172−5 °C; ^{1}H NMR 7.90 (1H, d, J = 8.56), 7.31 (2H, m), 6.99 (4H, m), 6.12 (1H, s), 3.93 (2H, s), 3.89 (3H, s), 3.76 (3H, s). $C_{18}H_{16}O_4$: C, H.

7-Methoxy-2-[(4′-methoxyphenyl)ethyl]-4*H*-1-benzopyran-4-one (12c) was synthesized by reaction between 2-hydroxy-4-methoxyacetophenone (**4b**) and methyl 4-methoxyphenylpropionate: yield 94%; mp 78−80 °C; ^{1}H NMR ($CDCl_3$) 8.10 (1H, d, J = 8.60), 7.15 (2H, m), 6.99 (1H, dd, J = 8.60, J = 2.30), 6.85 (3H, m), 6.10 (1H, s), 3.93 (3H, s), 3.81 (3H, s), 3.00 (2H, m), 2.90 (2H, m).

7-Methoxy-2-[(4′-methoxyphenyl)propyl]-4*H*-1-benzopyran-4-one (12d) was synthesized by reaction between 2-hydroxy-4-methoxyacetophenone **4b** and methyl 4-methoxyphenylbutanoate: yield 78%; mp 63−5 °C; ^{1}H NMR 7.90 (1H, d, J = 8.80), 7.15 (2H, m), 7.10 (1H, d, J = 2.42), 7.02 (1H, dd, J = 8.80, J = 2.42), 6.91 (2H, m), 6.15 (1H, s), 3.89 (3H, s), 3.72 (3H, s), 2.58 (4H, m), 1.99 (2H, m).

7-Methoxy-2-(3′,4′-dimethoxybenzyl)-4*H*-1-benzopyran-4-one (12e) was synthesized by reaction between 2-hydroxy-4-methoxyacetophenone (**4b**) and methyl 3,4-dimethoxyphenylacetate: yield 66%; mp 176−8 °C; ^{1}H NMR 7.90 (1H, d, J = 8.57), 6.98 (5H, m), 6.13 (1H, s), 3.93 (2H, s), 3.89 (3H, s), 3.77 (3H, s), 3.76 (3H, s).

7-Methoxy-2-(diphenylmethyl)-4*H*-1-benzopyran-4-one (12f) was synthesized by reaction between 2-hydroxy-4-methoxyacetophenone (**4b**) and methyl diphenylacetate: yield 59%; mp 146−8 °C; ^{1}H NMR 7.93 (1H, m), 7.34 (11H, m), 7.05 (2H, m), 5.97 (1H, s), 3.87 (3H, s).

7-Methoxy-2-[(2-naphthyl)methyl]-4*H*-1-benzopyran-4-one (12g) was synthesized by reaction between 2-hydroxy-4-methoxyacetophenone (**4b**) and methyl 2-naphthylacetate: yield 54%; mp 182−4 °C; ^{1}H NMR ($CDCl_3$) 8.12 (1H, d, J =

8.50), 7.90 (4H, m), 7.50 (3H, m), 6.98 (1H, dd, $J = 8.50$, $J = 2.40$), 6.82 (1H, d, $J = 2.40$), 6.18 (1H, s), 4.10 (2H, s), 3.88 (3H, s).

7-Methoxy-2-(4′-methoxybenzyl)-3-benzyl-4*H*-1-benzopyran-4-one (12h) was synthesized by reaction between 2′-hydroxy-4′-methoxydihydrochalcone (**4e**)[32] and methyl 4-methoxyphenylacetate: yield 25%; mp 108−10 °C; ^{1}H NMR ($CDCl_3$) 8.17 (1H, d, $J = 8.77$), 7.40 (5H, m), 7.15 (2H, m), 6.95 (1H, dd, $J = 8.77$, $J = 2.25$), 6.86 (2H, m), 6.80 (1H, d, $J = 2.25$), 4.09 (2H, s), 4.02 (2H, s), 3.91 (3H, s), 3.80 (3H, s).

7-Methoxy-2-(4′-methoxybenzyl)-3-[(1,1′-biphenyl-4-yl)-methyl]-4*H*-1-benzopyran-4-one (12i) was synthesized by reaction between 2′-hydroxy-4′-methoxy-4-phenyldihydrochalcone (**4f**) (prepared starting from biphenylcarboxaldehyde and 2-hydroxy-4-methoxyacetophenone following the general procedure described[32]) and methyl 4-methoxyphenylacetate: yield 7%; mp 101−2 °C; ^{1}H NMR ($CDCl_3$) 8.16 (1H, d, $J = 8.89$), 7.10 (15H, m), 4.07 (2H, s), 3.98 (2H, s), 3.89 (3H, s), 3.81 (3H, s).

7-Hydroxy-2-(4′-methoxybenzyl)-4*H*-1-benzopyran-4-one (12l) was synthesized by reaction between 2-hydroxy-4-(2-tetrahydropyranyloxy)acetophenone (**4g**)[49] and methyl 4-methoxyphenylacetate: yield 32%; mp 171−4 °C; ^{1}H NMR 10.69 (1H, s), 7.83 (1H d, $J = 8.72$), 7.31 (2H, m), 6.90 (3H, m), 6.78 (1H, d, $J = 2.20$), 6.03 (1H, s), 3.90 (2H, s), 3.76 (3H, s). $C_{17}H_{14}O_4$: C, H.

7-Hydroxy-2-benzyl-4*H*-1-benzopyran-4-one (12m) was synthesized by reaction between 2-hydroxy-4-(2-tetrahydropyranyloxy)acetophenone (**4g**)[49] and methyl phenylacetate: yield 40%; mp 167−9 °C; ^{1}H NMR ($CDCl_3$) 10.69 (1H, s), 7.84 (1H, d, 8.71), 7.32 (5H, m), 6.89 (1H, dd, $J = 8.70$, $J = 2.25$), 6.77 (1H, d, $J = 2.18$), 6.07 (1H, s), 3.98 (2H, s). $C_{16}H_{12}O_3$: C, H.

7-Bromo-2-(4′-methoxybenzyl)-4*H*-1-benzopyran-4-one (12n) was synthesized by reaction between 4-bromo-2-hydroxyacetophenone (**4h**)[50] and methyl 4-methoxyphenylacetate: yield 56%; mp 93−5 °C; ^{1}H NMR 7.92 (2H, m), 7.65 (1H, dd, $J = 1.80$, $J = 8.49$), 7.30 (2H, m), 6.92 (2H, m), 6.22 (1H, s), 3.96 (2H, s), 3.75 (3H, s).

7-[(Dimethylamino)methyl]-2-(4′-methoxybenzyl)-4*H*-1-benzopyran-4-one (12o). A solution of 1-(4-[(dimethylamino)methyl]-2-hydroxyphenyl)ethanone (**4i**)[51] (2.80 g, 14.5 mmol) and 4-methoxyphenylacetic acid methyl ester (2.88 g, 16.0 mmol) in anhydrous pyridine (8 mL) was added under stirring to a suspension of NaH (60% dispersion in mineral oil (2.08 g, 52.0 mmol) in anhydrous pyridine (5 mL). The reaction mixture was warmed to 100 °C for 20 min and then cooled, and anhydrous ether was added; the yellow precipitate was then collected and washed with diethyl ether. The solid was dissolved in acetic acid (30 mL), and concentrated HCl was added (1.5 mL). The resulting mixture was heated to 100 °C for 1 h; after cooling, the solvent was removed under reduced pressure and the resulting mixture was brought to pH 10.0 with NaOH, 5 N; the mixture was extracted with ethyl acetate (3 × 30 mL); the organic layers were dried (Na_2SO_4), and the solvent was removed under reduced pressure to afford an oil: yield 1.85 g (39.5%); ^{1}H NMR ($CDCl_3$) 8.12 (1H, d, $J = 8.05$), 7.42 (1H, d, $J = 1.0$), 7.35 (1H, dd, $J = 8.05$, $J = 1.0$), 7.40 (2H, m), 6.90 (2H, m), 6.13 (1H, s), 3.87 (2H, s), 3.83 (3H, s), 3.54 (2H, s), 2.29 (6H, s).

General Procedure for the Synthesis of Compounds 13a−m. To a stirred solution of **12a−i** (1.35 mmol) in anhydrous methylene chloride (30 mL) at 0 °C under N_2 atmosphere was added a BBr_3 solution in methylene chloride (4 equiv for **12f**,**g**, 5 equiv for **12a−d**,**h**,**i**, 6 equiv for **12e**); the solution was left to stand at room temperature for 24h, then it was cooled again to 0 °C, and water and ice were added. The resulting precipitate was collected and washed with water, then purified by column chromatography (methylene chloride: methanol, 96:4), and crystallized as described. Shortening the reaction time (3 h instead of 24 h) afforded compounds **13b**,**d** from **12a**,**b**, respectively.

6-Hydroxy-2-(4′-hydroxybenzyl)-4*H*-1-benzopyran-4-one (13a): from **12a**; yield 83%; mp 218−20 °C (acetone); ^{1}H NMR 9.91 (1H, s), 9.34 (1H, s), 7.45 (1H, d, $J = 8.94$), 7.28 (1H, d, $J = 2.94$), 7.16 (3H, m), 6.76 (2H, m), 6.08 (1H, s), 3.87 (2H, s). $C_{16}H_{12}O_4$: C, H.

6-Methoxy-2-(4′-hydroxybenzyl)-4*H*-1-benzopyran-4-one (13b): from **12a**; yield 61%; mp 148−50 °C (acetone); ^{1}H NMR 9.39 (1H, s), 7.54 (1H, m), 7.37 (2H, m), 7.18 (2H, m), 6.76 (2H, m), 6.15 (1H, s), 3.89 (2H, s), 3.84 (3H, s). $C_{17}H_{14}O_4$: C, H.

7-Hydroxy-2-(4′-hydroxybenzyl)-4*H*-1-benzopyran-4-one (13c): from **12b**; yield 83%; mp 258−60 °C (acetone/petroleum ether); ^{1}H NMR 10.70 (1H, s), 9.34 (1H, s), 7.84 (1H, d, $J = 8.71$), 7.16 (2H, m), 6.88 (1H, dd, $J = 8.71$, $J = 2.30$), 6.76 (3H, m), 6.00 (1H, s), 3.84 (2H, s). $C_{16}H_{12}O_4$: C, H.

7-Methoxy-2-(4′-hydroxybenzyl)-4*H*-1-benzopyran-4-one (13d): from **12b**; yield 14%; mp 188−90 °C (acetone); ^{1}H NMR 9.34 (1H, s), 7.88 (1H, d, $J = 8.60$), 7.17 (2H, m), 7.05 (2H, m), 6.78 (2H, m), 6.09 (1H, s), 3.90 (3H, s), 3.87 (2H, s). $C_{17}H_{14}O_4$: C, H.

7-Hydroxy-2-[(4′-hydroxyphenyl)ethyl]-4*H*-1-benzopyran-4-one (13e): from **12c**; yield 61%; mp 200−3 °C (acetone/petroleum ether); ^{1}H NMR 10.69 (1H, s), 9.15 (1H, s), 7.83 (1H, d, $J = 8.65$), 7.05 (2H, m), 6.89 (1H, dd, $J = 8.65$, $J = 2.24$), 6.82 (1H, d, $J = 2.24$), 6.68 (2H, m), 6.04 (1H, s), 2.88 (4H, s). $C_{17}H_{14}O_4$: C, H.

7-Hydroxy-2-[(4′-hydroxyphenyl)propyl]-4*H*-1-benzopyran-4-one (13f): from **12d**; yield 61%; mp 210−12 °C (acetone/petroleum ether); ^{1}H NMR 10.67 (1H, s), 9.11 (1H, s), 7.85 (1H, d, $J = 8.67$), 7.03 (2H, m), 6.89 (1H, dd, $J = 8.66$, $J = 2.22$), 6.83 (1H, d, $J = 2.09$), 6.82 (2H, m), 6.08 (1H, s), 2.57 (4H, m), 1.94 (2H, m). $C_{18}H_{16}O_4$: C, H.

7-Hydroxy-2-(3′,4′-dihydroxybenzyl)-4*H*-1-benzopyran-4-one (13g): from **12e**; yield 55%; mp 235−7 °C (acetone/petroleum ether); ^{1}H NMR 10.65 (1H, s), 8.80 (1H, s), 7.84 (1H, d, $J = 8.70$), 6.89 (1H, dd, $J = 8.71$, $J = 2.25$), 6.78 (1H, d, $J = 2.22$), 6.72 (2H, m), 6.60 (1H, m), 6.03 (1H, s), 3.78 (2H, s). $C_{16}H_{12}O_5$: C, H.

7-Hydroxy-2-(diphenylmethyl)-4*H*-1-benzopyran-4-one (13h): from **12f**; yield 53%; mp 255−8 °C (acetone); ^{1}H NMR 10.70 (1H, s), 7.87 (1H, d, $J = 8.71$), 7.36 (10H, m), 6.91 (1H, dd, $J = 8.79$, $J = 2.18$), 6.73 (1H, d, $J = 2.25$), 5.61 (1H, s). $C_{22}H_{16}O_3$: C, H.

7-Hydroxy-2-[(2-naphthyl)methyl]-4*H*-1-benzopyran-4-one (13i): from **12g**; yield 26%; mp 225−8 °C (acetone); ^{1}H NMR 10.67 (1H, s), 7.89 (5H, m), 7.53 (3H, m), 6.90 (1H, dd, $J = 8.71$, $J = 2.25$), 6.78 (1H, d, $J = 2.16$), 6.15 (1H, s), 3.29 (2H, s). $C_{20}H_{14}O_3$: C, H.

7-Hydroxy-2-(4′-hydroxybenzyl)-3-benzyl-4*H*-1-benzopyran-4-one (13l): from **12h**; yield 11%; mp 178−80 °C (acetone/petroleum ether); ^{1}H NMR 10.62 (1H, s), 9.26 (1H, s), 7.88 (1H, d, $J = 8.78$), 7.25 (5H, m), 7.01 (2H, m), 6.97 (1H, dd, $J = 8.78$, $J = 2.20$), 6.74 (1H, d, $J = 2.20$) 6.69 (2H, m), 3.94 (2H, s), 3.93 (2H, s). $C_{23}H_{18}O_4$: C, H.

7-Hydroxy-2-(4′-hydroxybenzyl)-3-[(1,1′-biphenyl-4-yl)-methyl]-4*H*-1-benzopyran-4-one (13m): from **12i**; yield 31%; mp 210−3 °C (acetone/petroleum ether); ^{1}H NMR 10.70 (1H, s), 9.25 (1H, s), 7.90 (1H, d, $J = 8.75$), 7.50 (9H, m), 7.00 (2H, m), 6.88 (1H, dd, $J = 8.75$), 6.75 (1H, d, $J = 2.24$), 6.66 (2H, m), 3.98 (4H, s). $C_{29}H_{22}O_4$: C, H.

7-Cyano-2-(4′-methoxybenzyl)-4*H*-1-benzopyran-4-one (14a). To a solution of **12n** (1.60 g, 4.64 mmol) in anhydrous DMF (10 mL) was added CuCN (0.45 g, 5.10 mmol). The reaction mixture was then heated at 150 °C for 3 h. After cooling, the reaction mixture was added to a solution of $FeCl_3$ (2.0 g) in water (40 mL) and the resulting mixture extracted with $CHCl_3$. Column chromatography (cyclohexane:AcOEt, 70:30) afforded 0.72 g (53%) of **14a**: mp 98 °C; ^{1}H NMR 8.30 (1H, d, $J = 1.50$), 8.11 (1H, d, $J = 8.14$), 7.85 (1H, dd, $J = J = 1.50$. $J = 8.14$), 7.35 (2H, m), 6.95 (2H, m), 6.30 (1H, s), 4.00 (2H, s), 3.76 (3H, s).

7-Cyano-2-(4′-hydroxybenzyl)-4*H*-1-benzopyran-4-one (14b). A solution of **14a** (0.66 g, 2.24 mmol) in methylene chloride (40 mL) at 0 °C was treated with BBr_3 (1 M solution in CH_2Cl_2) (11 mL, 11 mmol). The resulting solution was stirred at room temperature for 3 h and cooled at 0 °C, water

was added, the organic layer was dried (Na_2SO_4), and the solvent was removed under reduced pressure to obtain 0.50 g (80%) of compound **14b**: mp 192−5 °C; ^{1}H NMR 9.40 (1H, s), 8.26 (1H, d, J = 1.55), 8.13 (1H, d, J = 8.17), 7.85 (1H, dd, J = 8.17, J = 1.55), 7.20 (2H, m), 6.77 (2H, m), 6.28 (1H, s), 3.94 (2H, s).

7-Carboxy-2-(4′-hydroxybenzyl)-4*H*-1-benzopyran-4-one (14). 14b (0.35 g, 1.26 mmol) was dissolved in 70% H_2SO_4 (w/v) (10 mL) and heated at reflux for 90 min. Then the solution was cooled and poured into water and ice (80 mL). A dark solid formed which was washed with ethyl ether and then with acetone, to yield a white solid which was purified by crystallization from acetic acid/methanol: yield 0.105 g (28%); mp 273−6 °C; ^{1}H NMR 13.20 (1H, s), 9.30 (1H, s), 8.10 (1H, d, J = 8.16), 8.03 (1H, d, J = 1.50), 7.95 (1H, dd, J = 1.50, J = 8.18), 7.20 (2H, m), 6.75 (2H, m), 6.25 (1H, s), 3.93 (2H, s). $C_{17}H_{12}O_5$: C, H.

Acetic Acid 4-Methoxy-2-(3-propionyl)phenyl Ester (15b). Acetyl chloride (0.74 mL, 10.48 mmol) was added dropwise to a stirred solution of **15a**[32] (1.50 g, 5.24 mmol), triethylamine (3.5 mL, 25.1 mmol), and *N*,*N*-dimethylaminopyridine (0.070 g, 0.57 mmol) in methylene chloride (20 mL) at 0 °C. The reaction mixture was allowed to warm to ambient temperature for 1 h; then the volume was reduced in vacuo. The concentrate was diluted with EtOAc, washed with 1 N HCl and water, and then dried (Na_2SO_4), to give, after purification (column chromatography methanol:methylene chloride, 1:40 v/v), 1.47 g (85.5%) of **15b**, as an oil: ^{1}H NMR (acetone-d_6) 7.95 (1H, d, J = 8.77), 7.20 (2H, m), 6.93 (1H, dd, J = 2.57, J = 8.77), 6.87 (2H, m), 6.75 (1H, d, J = 2.57), 3.90 (3H, s), 3.79 (3H, s), 3.20 (2H, m), 2.91 (2H, m), 2.28 (3H, s).

7-Methoxy-2-methyl-3-(4′-methoxybenzyl)-4*H*-1-benzopyran-4-one (l5c). To a stirred suspension of NaH (60% dispersion in mineral oil) (0.70 g, 17.4 mmol), in DMSO (8 mL), at room temperature was added dropwise a solution of **15b** (1.87 g, 5.69 mmol) in DMSO (5 mL). The reaction mixture was stirred for 1 h at room temperature and then slowly poured into a ice/water mixture containing oxalic acid. The aqueous mixture was extracted with EtOAc, which in turn was washed with water, dried (Na_2SO_4), and evaporated in vacuo to give an oil. The oil was dissolved in acetic acid (25.0 mL) and concentrated HCl (1.5 mL) and then refluxed for 30 min. The reaction mixture was then poured into water and extracted with ethyl acetate, which was then washed with water, dried (Na_2SO_4), and purified (column chromatography methylene chloride:methanol, 95:5): yield 0.30 g (17%); mp 103−6 °C (acetone/petroleum ether); ^{1}H NMR 8.22 (1H, d, J = 8.67), 7.28 (2H, m), 7.05 (1H, dd, J = 8.67, J = 2.24), 6.90 (3H, m), 3.99 (3H, s), 3.96 (1H, s), 3.87 (3H, s), 2.50 (3H, s).

7-Hydroxy-2-methyl-3-(4′-hydroxybenzyl)-4*H*-1-benzopyran-4-one (15). The procedure was the same as reported for compound **13a**: yield 56%; mp 247−50 °C (acetone/petroleum ether); ^{1}H NMR ($CDCl_3$) 10.60 (1H, s), 9.00 (1H, s), 7.88 (1H, d, J = 8.74), 7.02 (2H, m), 6.85 (1H, dd, J = 2.24, J = 8.72), 6.78 (1H, d, J = 2.24), 6.65 (2H, m), 3 70 (2H, s), 2.38 (3H, s). $C_{17}H_{14}O_4$: C, H.

7-(Chloromethyl)-2-(4′-methoxybenzyl)-4*H*-1-benzopyran-4-one (16a). Ethyl chloroformate (1.67 mL, 17.5 mmol) was slowly added to a stirred solution of **12o** (1.88 g, 5.82 mmol) in benzene (15 mL) at 0 °C. A precipitate separated out which slowly dissolved. Stirring was continued at room temperature for 18 h, then water was added, the organic layer was washed twice with water and then dried (Na_2SO_4), and the solvent was removed under reduced pressure. The product was purified by column chromatography (cyclohexane:EtOAc, 62.5:37.5): yield 1.40 g (76.5%); mp 103−5 °C (CH_2Cl_2/EtOAc); ^{1}H NMR ($CDCl_3$) 8.17 (1H, d, J = 8.2), 7.48 (1H, d, J = 1.0), 7.37 (1H, dd, J = 8.2, J = 1.0), 7.42 (2H, m), 6.90 (2H, m), 6.15 (1H, s), 4.67 (2H, s), 3.89 (2H, s), 3.83 (3H, s).

7-(Cyanomethyl)-2-(4′-methoxybenzyl)-4*H*-1-benzopyran-4-one (16b). A solution of **16a** (0.50 g, 1.59 mmol) in DMSO (3 mL) was added to a suspension of KCN (0.13 g, 2.0 mmol) in anhydrous DMSO (2 mL) at 70 °C. The solution was stirred for 1 h at 80 °C, then poured into cold water, and extracted with ethyl acetate (3 × 50 mL). The organic layer was dried (Na_2SO_4), the solvent was removed under reduced pressure, and the residue was purified by column chromatography (cyclohexane:EtOAc, 62.5:37.5): yield 0.070 g (14%); mp 107−9 °C; ^{1}H NMR ($CDCl_3$) 8.15 (1H, d, J = 8.15), 7.47 (1H, d, J = 1.0), 7.25 (3H, m), 6.90 (2H, m), 6.14 (1H, s), 3.88 (4H, s), 3.82 (3H, s).

7-(Cyanomethyl)-2-(4′-hydroxybenzyl)-4*H*-1-benzopyran-4-one (16c). A solution of BBr_3 in CH_2Cl_2 (1 M, 0.91 mL, 0.91 mmol) was added to a solution of **16b** (0.070 g, 0.23 mmol) in methylene chloride (10 mL) at 0 °C. Stirring was continued for 3 h at room temperature, then the reaction mixture was cooled, water was added, and the aqueous layer was extracted with CH_2Cl_2 (2 × 5 mL). The combined organic layers were dried (Na_2SO_4), the solvent was removed under reduced pressure, and the residue was crystallized from acetone: yield 0.030 g (45%); mp 190−3 °C dec; ^{1}H NMR 8.05 (1H, d, J = 8.10), 7.57 (1H, d, J = 1.0), 7.45 (1H, dd, J = 8.10, J = 1.0), 7.15 (2H, m), 6.75 (2H, m), 6.21 (1H, s), 4.80 (1H, broad s), 4.24 (2H, s), 3.91 (2H, s).

7-Acetyl-2-(4′-hydroxybenzyl)-4*H*-1-benzopyran-4-one (16). A solution of **16c** (0.030 g, 0.10 mmol) in 70% H_2SO_4 (w/v) (2 mL) was heated at 130 °C for 2 h; then the solution was cooled and poured into ice-cold water (8 mL). The oily residue was purified on TLC (cyclohexane/EtOAc/acetic acid, 25/75/1) and crystallized from acetone/petroleum ether: yield 0.06 g (19%); mp 218−20 °C; ^{1}H NMR (acetone-d_6) 11.00 (1H, broad s), 8.39 (1H, s), 8.02 (1H, d, J = 8.05), 7.52 (1H, d, J = 1.4), 7.40 (1H, dd, J = 8.05, J = 1.4), 7.27 (2H, m), 6.85 (2H, m), 6.13 (1H, s), 3.95 (2H, s), 3.86 (2H, s). $C_{18}H_{14}O_5$: C, H.

7-Hydroxy-3-(4′-hydroxybenzyl)-4*H*-1-benzopyran-4-one (17). Boron trifluoride−diethyl etherate (0.98 mL, 7.75 mmol) was added dropwise to a solution of 2′,4,4′-trihydroxydihydrochalcone[32] (0.50 g, 1.94 mmol) in anhydrous DMF (5 mL) at 10 °C. Methanesulfonyl chloride (0.45 mL, 5.81 mmol) was then added and the solution heated at 50 °C for 90 min. After cooling, water was added and the mixture was extracted with methylene chloride (2 × 25 mL) and then with ethyl acetate (2 × 25 mL). After the combined organic layers were dried (Na_2SO_4), the solvents were removed under reduced pressure and the residue was purified by column chromatography (cyclohexane/EtOAc, 50/50): yield 0.28 g (54%); mp 205−6 °C (acetone/petroleum ether); ^{1}H NMR 10.69 (1H, s), 9.13 (1H, s), 8.09 (1H, s), 7.88 (1H, d, J = 8.72), 7.10 (2H, m), 6.91 (1H, dd, J = 8.72, J = 2.27), 6.83 (1H, d, J = 2.12), 6.67 (2H, m), 3.56 (2H, s). $C_{16}H_{12}O_4$: C, H.

7-Methoxy-3-(4′-hydroxybenzyl)-4*H*-1-benzopyran-4-one (18). An ethereal solution of diazomethane was added to a solution of **17** (0.050 g, 0.19 mmol) in absolute methanol (50 mL) at 0 °C until the solution became slightly yellow; the solvent was then removed under reduced pressure and the residue crystallized from acetone/petroleum ether: yield 0.020 g (38%); ^{1}H NMR 9.12 (1H, s), 8.16 (1H, s), 7.95 (1H, d, j 8.78), 7.10 (4H, m), 6.63 (2H, m), 3.90 (3H, s), 3.59 (2H, s). $C_{17}H_{14}O_4$: C, H.

Determination of the Proton Dissociation Constants (pK_a). The compounds being studied were dissolved in DMSO at a concentration of about 3.5 mM. Samples (15 μL) of this solution were each added to 3 mL of buffer at a constant ionic strength[52] (I = 0.1 M) and with pH increasing each time in increments of 0.25 unit; UV−vis spectra were recorded, and the pH of the solution was measured with a combined electrode (Orion SA 520) calibrated with buffers at pH 4.01, 7.00, and 10.01. The numerical values of the proton dissociation constants of the compounds under study were calculated from the change in absorbance at the maximum λ of the dissociated forms following the procedure reported in ref 53; pK_a values were then corrected for ionic strength as described therein.[53]

Antilipoperoxidant Assay. 1. AAPH-Induced Peroxidation of Liposomes. Linoleic acid (LA) was purchased from Sigma, 2,6-di-*tert*-butyl-*p*-cresol (BHT) from Schuchardt (Munchen, Germany), and 2,2′-azobis(2-aminopropane) hydrochloride (AAPH) from Polysciences, Inc. (Warrington, PA). **13a**,**c**,**g** and BHT were dissolved in THF and evaporated to

dryness under nitrogen. The LA (2 mg/mL) was added and suspended by simple vortexing in Tris buffer (50mM), pH 7.4. This suspension was then processed through a Thermobarrel Extruder (Lipex Biomembranes Inc., Vancouver, Canada) to form micelles in which the final concentration of antioxidants was 0.2 mM. The antioxidant activity of the compounds was assessed by evaluating the AAPH-induced malondialdehyde (MDA) production in micelles. The MDA was measured by the thiobarbituric acid (TBA) test in antioxidant-containing micelles incubated with AAPH (10 mM) at 37 °C in a shaking waterbath. Aliquots (0.7 mL) of the micelles in suspension were removed at regular intervals, and an equivalent amount of 20% TCA was added; 1 mL of this mixture was added to 1 mL of 0.67% TBA. The solution was heated for 10 min in a boiling waterbath and then cooled in ice-cold water. Samples were then processed through an equivalent amount of hexane to extract the lipids. The pink aqueous phase, containing the MDA, was then separated from the hexane layer by centrifugation at 2.000*g* for 15 min and the MDA measured at the spectrophotometer at 535 nm, using a molar absorption coefficient (ϵ) = 1.49×10^5 (L mol^{-1} cm^{-1}).[54] The data are expressed as means ± SE. Significance was estimated using Student's two-tailed *t*-test; the criterion for significance was $p < 0.01$.

2. VLDL + LDL Lipoprotein Oxidation Model.[55] LDL + VLDL lipoproteins were isolated from the plasma of a normocholesterolemic subject by means of affinity chromatography (Iso-Lab Inc., Akron, OH). Protein content (Coomassie Blue, Sigma, albumin as standard) was adjusted to 70 μg/mL using phosphate buffer (pH 7.40). Cupric ions were added as oxidant at 25 μM in a total volume of 400 μL. Oxidation was continued for 6 h at 37 °C and then halted by the addition of 10 μL of 10 mM EDTA and 1 mL of 10% trichloroacetic acid; 1 mL of thiobarbituric acid (TBA) (0.67 g/100 mL) was then added and the samples were heated at 95 °C for 2 h. The fluorescence of TBA-reactive substances was read at 525 nm excitation and 554 nm emission versus a blank. A control sample with no added antioxidants was measured along with the compounds tested, which were dissolved in methanol (100 μM) and added to the incubation mixture at concentrations ranging from 0.05 to 10 μM. All samples and controls were measured in duplicate (differences between duplicates within 10%). The percent inhibition of the samples versus the control was determined, and the concentration required to inhibit oxidation by 50% (IC_{50}) was calculated.

Enzyme Section. Bovine lenses and kidneys for the purification of ALR2 and ALR1, respectively, were obtained locally from freshly slaughtered animals. ALR2 was partially purified as described.[30] Briefly, the bovine lenses were suspended in sodium phosphate buffer (pH 7.00), containing 5 mM dithiothreitol. After centrifugation at 22.000*g* at 4 °C for 20 min; the supernatant was subjected to ion-exchange chromatography (DEAE DE52), eluted with a linear gradient of NaCl, and stored at −20 °C. ALR1 was partially purified following the procedure reported in the literature.[30] Briefly, bovine kidneys were homogenized in 3 vol of 0.25 M sucrose, 2.0 mM EDTA dipotassium salt, and 2.5 mM β-mercaptoethanol in 10 mM sodium phosphate buffer (pH 7.20). The homogenate was centrifuged (16.000*g* at 4 °C for 20 min) and the supernatant subjected to ammonium sulfate fractional precipitation. The pellet obtained between 45% and 75% of salt saturation was redissolved in 10 mM sodium phosphate buffer containing 2.0 mM EDTA dipotassium salt and 2.0 mM β-mercaptoethanol at a protein concentration of approximatively 20 mg/mL; DEAE DE52 resin was added to the solution and then removed by centrifugation; the supernatant containing ALR1 was then stored at −20 °C. No appreciable contamination by ALR1 in ALR2 preparations or vice versa could be detected as is clear from the K_m values for D-glucose (ALR2, K_m 25.1 ± 1.9 mM; ALR1, no activity at up to 150 mM) and the IC_{50} values for Valproate (ALR2, IC_{50} 61.7 (57.4−66.3) μM; ALR1, IC_{50} 2.01 (1.37−2.93) μM).[56]

The assay for ALR2 activity was performed at 37 °C as described, using 4.7 mM D,L-glyceraldehyde as substrate in 0.25 M sodium phosphate buffer (pH 6.80), containing 0.38 M ammonium sulfate and 0.11 mM NADPH. ALR1 activity was assayed at 37 °C using 20 mM D-glucuronate as substrate and 0.12 mM NADPH in 0.1 M sodium phosphate buffer (pH 7.20). The inhibitory activity against ALR2 and ALR1 of the compounds was tested by including the inhibitor dissolved in DMSO in the reaction mixture. DMSO in the assay mixture was kept at a constant concentration of 1%. A reference blank containing all the above reagents, except the substrate, was used to correct for the nonenzymatic oxidation of NADPH. The enzyme concentrations in the inhibitory study were 3.5 mU/mL for both enzymes. IC_{50} values (the concentration of the inhibitor required to produce 50% inhibition of the enzyme-catalyzed reaction) were determined from least-squares analyses of the linear portion of the log dose−inhibition curves. Each curve was generated using at least four concentrations of inhibitor causing an inhibition between 20% and 80% with two replicates at each concentration.[30] The 95% confidence limits (95% CL) were calculated from *T* values for $n - 2$, where *n* is the total number of determinations.[57]

Computational Procedures. The geometries of the inhibitors were completely optimized using the AM1 Hamiltonian. Inhibitors **13c** and **4** were considered dissociated at the 7-hydroxyl on account of the low pK_a value of this hydroxyl, and inhibitor **3** was dissociated at the 7-acetic acid group. For inhibitors **13c** and **16**, which possess a methyl spacer at position 2 between benzopyrone and phenyl, the two conformations in which the phenyl ring is rotated by ±90° with respect to benzopyrone were both optimized with AM1.

The two structures of ALR2 used for docking and molecular mechanics calculations are the crystal structure of the ALR2−$NADP^+$ holoenzyme[41] (closed structure of the hydrophobic pocket described in the text) and the ALR2 structure that we previously obtained after docking and energy minimization of a bulky inhibitor in the active site (open structure of the hydrophobic pocket). [38]

Docking of inhibitors was performed using the program DOCK 3.5,[58] which consists of several modules. The module SPHGEN[59] was used to generate clusters of overlapping spheres that describe the accessible surface of the active site; 52 and 74 spheres were used to describe the active sites of the closed and open structures of ALR2, respectively. The module CHEMGRID[60] was then used to precompute and save in a grid file the information necessary for force-field scoring. This scoring function approximates molecular mechanics interaction energies and consists of van der Waals and electrostatic components.[60]As for inhibitors **13c**, **4**, and **16**, partial charges on atoms were calculated with electrostatic potential fits to a 6-31G* ab initio wave function using Gaussian94, followed by a standard RESP[61,62] fit. These charges were also used for the molecular mechanics calculations described below. van der Waals parameters of inhibitors were set consistently with the DOCK database.[60] The program DOCK 3.5 was then run to find and score orientations of the inhibitors in the active site. Each orientation of each ligand was filtered for steric fit with a DISTMAP grid[63] with polar and nonpolar contact limits of 2.3 and 2.8 Å, respectively. Orientations that passed this steric filter were evaluated for van der Waals and electrostatic complementarity using the grids calculated by CHEMGRID.

All orientations within a 10 kcal/mol range of interaction energy from the best scoring orientation found by DOCK were visually inspected using the computer graphics program MidasPlus[64] and found to cluster into families. Each significantly different orientation, representing each family, was then energy-minimized with molecular mechanics. The AMBER 4.1[65] program with the Cornell et al.[66] force field was used for this purpose. van der Waals parameters of the inhibitors were reassigned to be consistent with the Cornell force field, and partial atomic charges were the same as those used for DOCK. Parameters for $NADP^+$ were taken from our previous simulations.[29,30,38] As for ALR2, all Lys and Arg residues were positively charged, while Glu and Asp residues were negatively charged; the δH, ϵH or protonated forms of histidines were

assigned on the basis of favorable interactions with their environment. His110, a histidine involved in the binding of inhibitors,[27,28] deservers particular mention. Previous modeling studies by Lee et al.[67,68] suggested that this histidine is protonated mainly on account of its close proximity to the carboxylate group of Zopolrestat in the crystal structure of the complex with ALR2.[27] However, X-ray crystallography at 1.8 Å resolution is not able to assign its protonation state unambiguously. On the contrary, there are pieces of experimental evidence from pH-dependent kinetic profiles and mutagenesis studies that His110 is likely to be neutral at physiological pH.[39,69−71] These studies indicate that the pronounced hydrophobic nature of the region surrounding His110 and its proximity to the positively charged Lys77 would serve to depress the pK_a of the imidazole side chain, making it unlikely to be protonated. Recent modeling studies of substrates in the ALR2 binding site would also suggest that His110 is not protonated.[42] Accordingly, in the present work, His110 was modeled as neutral in its ϵH tautomeric form, i.e., with the ϵH proton directed toward the inhibitory binding cleft.

Conjugate gradient minimization (2000 steps) was then performed. All protein residues within 10 Å from the inhibitor were allowed to move during minimization. A distance-dependent dielectric constant with a 4*r* dependence and a 10 Å nonbonded cutoff were adopted in all simulations. Interaction energies of the inhibitors with ALR2 were recalculated using the optimized structures and the Cornell force field, using the module ANAL of AMBER 4.1. Calculations and graphical display were performed on Silicon Graphics O2 workstations.

References

(1) Larson, E. R.; Lipinski, C. A.; Sarges, R. Medicinal chemistry of aldose reductase inhibitors. *Med. Res. Rev*. **1988**, *8*, 159−186.

(2) Eggler, J. F.; Larson, E. R.; Lipinski, C. A.; Mylari, B. L.; Urban, F. J. A perspective of aldose reductase inhibitors. *Advances In Medical Chemistry*; Jai Press: Greenwich, CT, 1993; Vol. 2, pp 197−246.

(3) Sarges, R.; Oates, P. J. Aldose reductase inhibitors: recent developments. *Prog. Drug Res.* **1993**, *40*, 99−161.

(4) Costantino, L.; Rastelli, G.; Cignarella, G.; Vianello, G.; Barlocco, D. New aldose reductase inhibitors as potential agents for the prevention of long-term diabetic complications. *Exp. Opin. Ther. Patents* **1997**, *7*, 843−858.

(5) Porte, D.; Schwartz, M. W. Diabetes complications: why is glucose potentially toxic? *Science* **1996**, *272*, 699−700.

(6) Baynes, J. W. Role of oxidative stress in development of complications in diabetes. *Diabetes* **1991**, *40*, 405−412.

(7) Traverso, N.; Menini, S.; Odetti, P.; Pronzato, M. A.; Cottalasso, D.; Marinari, U. M. Diabetes affect lipid peroxidation in hepatic subcellular compartments. Society for Free Radical Research 1997, Summer Meeting, June 26−28, 1997, Abano Terme, Padova, Italy; Abstr. Book, p 77.

(8) Traverso, N.; Menini, S.; Cosso, L.; Odetti, P.; Albano, E.; Pronzato, E.; Marinari, U. M. Immunological evidence for increased oxidative stress in diabetic rats. *Diabetologia* **1998**, *41*, 265−270.

(9) Esterbauer, H.; Schaur, R. J.; Zollner, H. Chemistry and biochemistry of 4-hydroxynonenal, malonaldehyde and related aldehydes. *Free Radical Biol. Med.* **1991**, *11*, 81−128.

(10) Vander Jagt, D. L.; Kolb, N. S.; Vander Jagt, T. J.; Chino, J.; Martinez, F.; Hunsaker, L. A.; Royer, R. E. Substrate specificity of human aldose reductase: identification of 4-hydroxynonenal as an endogenous substrate. *Biochim. Biophys. Acta* **1995**, *1249*, 117−126.

(11) Srivastava, S.; Chandra, A.; Bhatnagar, A.; Srivastava, S. K.; Ansari, N. H. Lipid peroxidation product, 4-hydroxynonenal and its conjugate with GSH are excellent substrates of bovine lens aldose reductase. *Biochem. Biophys. Res. Commun*. **1995**, *217*, 741−746.

(12) Kador, P. F.; Kinoshita, J. H.; Brittain, D. R.; Mirrlees, D. J.; Sennitt, C. M.; Stribling, D. Purified rat lens aldose reductase. Polyol production in vitro and its inhibition by aldose reductase inhibitors. *Biochem. J*. **1986**, *240*, 233−237.

(13) Spycher, S.; Tabataba-Vakili, S.; O'Donnell, V. B.; Palomba, L.; Azzi, A. 4-hydroxy-2,3-trans-nonenal induces transcription and expression of aldose reductase. *Biochem. Biophys. Res. Commun*. **1996**, *226*, 512−516.

(14) Spycher, S. E.; Tabataba-Vakili, S.; O'Donnell, V. B.; Palomba, L.; Azzi, A. Aldose reductase induction: a novel response to oxidative stress of smooth muscle cells. *FASEB J*. **1997**, *11*, 181−188.

(15) Ansari, N. H.; Wang, L.; Srivastava, S. K. Role of lipid aldehydes in cataractogenesis: 4-hydroxynonenal-induced cataract. *Biochem. Mol. Med*. **1996**, *58*, 25−30.

(16) Cappiello, M.; Voltarelli, M.; Cecconi, I.; Vilardo, P. G.; Dal Monte, M.; Marini, I.; Del Corso, A.; Wilson, D. K.; Florante, A. Q.; Petrash, J. M.; Mura, U. Specifically targeted modification of human aldose reductase by physiological disulfides. *J. Biol. Chem*. **1996**, *271*, 33539−33544.

(17) Grimshaw, C. E.; Lai, C. J. Oxidized aldose reductase: in vivo factor, not in vitro artifact. *Arch. Biochem. Biophys*. **1996**, *327*, 89−97.

(18) Cappiello, M.; Vilardo, P. G.; Cecconi, I.; Leverenz, V.; Giblin, F. J.; Del Corso, A.; Mura, U. Occurrence of glutathione-modified aldose reductase in oxidatively stressed bovine lens. *Biochem. Biophys. Res. Commun*. **1995**, *207*, 775−782.

(19) Middleton, E.; Kandaswami, C. The impact of plant flavonoids on mammalian biology: implications for immunity, inflammation and cancer. In *The flavonoids, Advances in Research since 1986*; Harborne, J.B., Ed.; Chapman and Hall: London, 1994; pp 619−652.

(20) Varma, S. D.; Kinoshita, J. H. Inhibition of lens aldose reductase by flavonoids. Their possible role in the prevention of diabetic cataracts. *Biochem. Pharmacol*. **1976**, *25*, 2505−2513.

(21) Kador, P. F.; Sharpless, N. E. Structure−activity studies of aldose reductase inhibitors containing the 4-oxo-4*H*-chromen ring system. *Biophys. Chem*. **1978**, *8*, 81−85.

(22) Okuda, J.; Miwa, I.; Inagaki, K.; Horie, T.; Nakayama, M. Inhibition of aldose reductases from rat and bovine lenses by flavonoids. *Biochem. Pharmacol*. **1982**, *31*, 3807−3822.

(23) Chaudhry, P. S.; Cabrera, J.; Juliani, H. R.; Varma, S. D. Inhibition of human lens aldose reductase by flavonoids, sulindac and indomethacin. *Biochem. Pharmacol*. **1983**, *32*, 1995−1998.

(24) Kador, P. F.; Sharpless, N. E. Pharmacophor requirements of the aldose reductase inhibitor site. *Mol. Pharmacol*. **1983**, *24*, 521−531.

(25) Okuda, J.; Miwa, I.; Inagaki, K.; Horie, T.; Nakayama, M. Inhibition of aldose reductase by 3′,4′-dihydroxyflavones. *Chem. Pharm. Bull*. **1984**, *32*, 767−772.

(26) Iinuma, M.; Tanaka, T.; Mizuno, M.; Katsuzaki, T.; Ogawa, H. Structure−activity correlation of flavonoids for inhibition of bovine lens aldose reductase. *Chem. Pharm. Bull*. **1989**, *37*, 1813−1815.

(27) Wilson, D. K.; Tarle, I.; Petrash, J. M.; Quiocho, F. A. Refined 1.8 A structure of human aldose reductase complexed with the potent inhibitor zopolrestat. *Proc. Natl. Acad. Sci. U.S.A*. **1993**, *90*, 9847−9851.

(28) Urzhumtsev, A.; Tete-Favier, F.; Mitscler, A.; Barbanton, J.; Barth, P.; Urzhumgtseva, L.; Biellmann, J. F.; Podjarny, A. D.; Moras, D. A 'specificity' pocket inferred from the crystal structures of the complexes of aldose reductase with the pharmaceutically important inhibitors tolrestat and sorbinil. *Structure* **1997**, *5*, 601−612.

(29) Rastelli, G.; Costantino, L. Molecular dynamics simulations of the structure of aldose reductase complexed with the inhibitor tolrestat. *Bioorg. Med. Chem. Lett*. **1998**, *8*, 641−646.

(30) Costantino, L.; Rastelli, G.; Vescovini, K.; Cignarella, G.; Vianello, P.; Del Corso, A.; Cappiello, M.; Mura, U.; Barlocco, D. Synthesis, activity, and molecular modeling of a new series of tricyclic pyridazinones as selective aldose reductase inhibitors. *J. Med. Chem*. **1996**, *39*, 4396−4405.

(31) Cushman, M.; Nagarathnam, D. A method for the facile synthesis of ring-A hydroxylated flavones. *Tetrahedron Lett*. **1990**, *31*, 6497−6500.

(32) Shantanu, D. E.; Vimal, N. J.; Krishnamurty, H. G. A simple and efficient conversion of chalchones to dihydrochalchones. *Indian J. Chem*. **1994**, *33B*, 163−165.

(33) Bass, R. J. Synthesis of chromones by cyclization of 2-hydroxyphenyl ketones with boron trifluoride-diethyl ether and methane sulphonyl chloride. *J. Chem. Soc., Chem. Commun*. **1976**, 78−79.

(34) Costantino, L.; Rastelli, G.; Albasini, A. A rational approach to the design of flavones as xanthine oxidase inhibitors. *Eur. J. Med. Chem*. **1996**, *31*, 693−699.

(35) Tyukavkina, N. A.; Pogodaeva, N. N. Ultraviolet absorption of flavonoids III. Ionization constants of the 5-hydroxy group in 5,N-dihydroxy flavones. *Khim. Prir. Soedin*. **1972**, *2*, 173−176.

(36) Wolfbeis, O. S.; Leiner, M.; Hochmuth, P.; Geiger, H. Absorption and fluorescence spectra, pK_a values, and fluorescence lifetimes of monohydroxyflavones and monomethoxyflavones. *Ber. Bunsen-Ges. Phys. Chem*. **1984**, *88*, 759−767.

(37) Vinson, J. A.; Dabbagh, Y. A.; Serry, M. M.; Jang, J. Plasnt flavonoids, especially tea flavonoids, are powerful antioxidants using an in vitro oxidation model for heart disease. *J. Agric. Food Chem*. **1995**, *43*, 2800−2802.

(38) Rastelli, G.; Vianello, P.; Barlocco, D.; Costantino, L.; Del Corso, A.; Mura, U. Structure-based design of an inhibitor modeled at the substrate active site of aldose reductase. *Bioorg. Med. Chem. Lett*. **1997**, *7*, 1897−1902.

(39) Bohren, K. M.; Grimshaw, C. E.; Lai, C. J.; Harrison, D. H.; Ringe, D.; Petsko, G. A.; Gabbay, K. H. Tyrosine-48 is the proton donor and histidine-110 directs substrate stereochemical selectivity in the reduction reaction of human aldose reductase: enzyme kinetics and crystal structure of the Y48H mutant enzyme. *Biochemistry* **1994**, *33*, 2021−2032.
(40) Grimshaw, C. E.; Bohren, K. M.; Lai, C. J.; Gabbay, K. H. Human aldose reductase: p*K* of tyrosine 48 reveals the preferred ionization state for catalysis and inhibition. *Biochemistry* **1995**, *34*, 14374−14384.
(41) Wilson, D. K.; Bohren, K. M.; Gabbay, K. H.; Quiocho, F. A. An unlikely sugar substrate in the 1.65 A structure of the human aldose reductase holoenzyme implicated in diabetic complications. *Science* **1992**, *257*, 81−84.
(42) De Winter, H. L.; von Itzstein, M. Aldose reductase as a target for drug design: molecular modeling calculations on the binding of acyclic sugar substrates to the enzyme. *Biochemistry* **1995**, *34*, 8299−8308.
(43) El-Kabbani, O.; Carper, D. A.; McGowan, M. H.; Devedjiev, Y.; Milton, K. J.; Flynn, T. G. Studies on the inhibitor-binding site of porcine aldehyde reductase: crystal structure of the holoenzyme−inhibitor ternary complex. *Proteins* **1997**, *28*, 186−192.
(44) Jaen, J. C.; Wise, L. D.; Heffner, T. G.; Pugsley, T. A.; Meltzer, L. T. Dopamine autoreceptor agonists as potential antipsycotics. 2. (Aminoalkoxy)-4*H*-1-benzopyran-4-ones. *J. Med. Chem.* **1991**, *34*, 248−256.
(45) Beilstein, 18, IV, 693.
(46) Fitgerald, D. M.; O'Sullivan, J. F.; Philbin, E. M.; Wheeler, T. S. Ring expansion of 2-benzylidencoumaran-3-ones. A synthesis of flavones. *J. Chem. Soc.* **1955**, 860−862.
(47) Mahal, H. S.; Rai, H. S.; Venkantamaran, K. Synthetical experiments in the chromone group. Part XVI. Chalkones and flavanones and their oxidation to flavones by means of selenium dioxide. *J. Chem. Soc.* **1935**, 866−868.
(48) Cushman, M.; Zhu, H.; Geahlen, R. L.; Kraker, A. J. Synthesis and biochemical evaluation of a series of aminoflavones as potential inhibitors of protein-tyrosine kinase $P56^{lkc}$, EGFr and $p60^{v-src}$. *J. Med. Chem.* **1994**, *37*, 3353−3362.
(49) Sogawa, S.; Nihro, Y.; Ueda, H.; Miki, T.; Matsumoto, H.; Satoh, T. Protective effects of hydroxychalkones on free radical-induced cell damage. *Biol. Pharm Bull.* **1994**, *17*, 251−256.
(50) Chen, F. C.; Chang, C. T. Synthesis of 7-halogenoflavones and related compounds. *J. Chem. Soc.* **1958**, 146−150.
(51) Dillard, R. D.; Carr, F. P.; McCullough, D.; Haisch, K. D.; Rinkema, L. E.; Fleisch, J. H. Leukotriene receptor antagonists. 2. The (((tetrazol-5-ylaryl)oxy)methyl)acetophenone derivatives. *J. Med. Chem.* **1987**, *30*, 911−918.
(52) Miller, G. L.; Golder, R. H. Buffers of pH 2 to 12 for use in electrophoresis. *Arch. Biochem.* **1950**, *29*, 420−423.
(53) Albert, A. *The determination of ionization constants*, 3rd ed.; Methuen Co. Ltd., 1984.
(54) Slater, T. F.; Sawyer, B. C. The stimulatory effect of carbon tetrachloride and other halogenoalkanes on peroxidative reaction in rat liver fractions in vitro. *Biochem. J.* **1971**, *123*, 805−814.
(55) Vinson, J. A.; Hontz, B. A. Phenol antioxidant index: comparative antioxidant effectiveness of red and white wines. *J. Agric. Food Chem.* **1995**, *43*, 401−403.
(56) Ward, W. H. J.; Sennitt, C. M.; Ross, H.; Dingle, A.; Timms, D.; Mirrlees, D. J.; Tuffin, D. P. Ponalrestat: a potent and specific inhibitor of aldose reductase. *Biochem. Pharmacol.* **1990**, *39*, 337−346.
(57) Tallarida, R. J.; Murray, R. B. *Manual of pharmacological calculations with computer programs*, 2nd ed.; Springer-Verlag: New York, 1987.
(58) Gschwend, D. A.; Kuntz, I. D. Orientational sampling and rigid-body minimization in molecular docking revisited: on-the-fly optimization and degeneracy removal. *J. Comput.-Aided Mol. Des.* **1996**, *10*, 123−132.
(59) Kuntz, I. D.; Blaney, J. M.; Oatley, S. J.; Langridge, R.; Ferrin, T. E. A geometric approach to macromolecule-ligand interactions. *J. Mol. Biol.* **1982**, *161*, 269−288.
(60) Meng, E. C.; Shoicket, B. K.; Kuntz, I. D. Automated docking with Grid-based energy evaluation. *J. Comput. Chem.* **1992**, *13*, 505−524.
(61) Bayly, C. I.; Cieplak, P.; Cornell, W. D.; Kollman, P. A. A well-behaved electrostatic potential based method using charge restraints for deriving atomic charges: the RESP model. *J. Phys. Chem.* **1993**, *97*, 10269−10280.
(62) Cieplak, P.; Bayly, C. I.; Cornell, W. D.; Kollman, P. A. Application of the multimolecule and multiconformational RESP methodology to byopolymers: charge derivation for DNA, RNA, and proteins. *J. Comput. Chem.* **1995**, *16*, 1357−1377.
(63) Shoicket, B. K.; Bodian, D. L.; Kuntz, I. D. Molecular docking using shape descriptors. *J. Comput. Chem.* **1992**, *13*, 380−397.
(64) Ferrin, T. E.; Huang, C. C.; Jarvis, L. E.; Langridge, R. The MIDAS display system. *J. Mol. Graph.* **1988**, *6*, 13−27.
(65) Pearlman, D. A.; Case, D. A.; Caldwell, J. W.; Ross, W. S.; Cheatman III, T. E.; Ferguson, D. M.; Seibel, G. L.; Singh, U. C.; Weiner, P. K.; Kollman, P. A. *AMBER 4.1*; University of California: San Francisco, 1995.
(66) Cornell, W. D.; Cieplak, P.; Bayly, C. I.; Gould, I. R.; Merz, K. M., Jr.; Ferguson, D. M.; Spellmeyer, D. C.; Fox, T.; Caldwell, J. W.; Kollman, P. A. A second generation force-field for the simulation of proteins, nucleic acids, and organic molecules. *J. Am. Chem. Soc.* **1995**, *117*, 5179−5197.
(67) Lee, Y. S.; Chen, Z.; Kador, P. F. Molecular modeling studies of the binding modes of aldose reductase inhibitors at the active site of human aldose reductase. *Bioorg. Med. Chem.* **1998**, *6*, 1811−1819.
(68) Lee, Y. S.; Hodoscek, M.; Brooks, B. R.; Kador, P. F. Catalytic mechanism of aldose reductase studied by the combined potentials of quantum mechanics and molecular mechanics. *Biophys. Chem.* **1998**, *70*, 203−216.
(69) Petrash, J. M.; Tarle, I.; Wilson, D. K.; Quiocho, F. A. Aldose reductase catalysis and crystallography. Insight from recent advances in enzyme structure and function. *Diabetes* **1994**, *43*, 955−959.
(70) Harrison, D. H.; Bohren, K. M.; Ringe, D.; Petsko, G. A.; Gabbay, K. H. An anion binding site in human aldose reductase: mechanistic implications for the binding of citrate, cacodylate, and glucose-6-phosphate. *Biochemistry* **1994**, *33*, 2011−2020.
(71) Ehrig, T.; Bohren, K. M.; Prendergast, F. G.; Gabbay, K. H. Mechanism of aldose reductase inhibition: binding of $NADP^+$/NADPH and alrestatin-like inhibitors. *Biochemistry* **1994**, *33*, 7157−7165.

JM980441H